A Diverse Array of C-C Bonds Formed at a

Tantalum Metal Center

Jade I. Fostvedt, Michael A. Boreen, Robert G. Bergman* and John Arnold*

Department of Chemistry, University of California, Berkeley, CA, 94720, United States

ABSTRACT. We demonstrate the formation of a diverse array of organic and organometallic products containing newly-formed C-C bonds via successive methyl transfers from di-, tri-, and tetramethyl Ta(V) precursors to unsaturated small molecule substrates under mild conditions. The reactions of Ta(V) methyl complexes **1-X** [H₂B(Mes Im)₂]TaMe₃X (X = Me, Cl; Im = imidazole, Mes = 2,4,6-trimethylphenyl) with CO led to oxo enolate Ta(V) products, in which the enolate ligands were constructed from Ta-Me groups and two equivalents of CO. Similarly, the reaction of **1-Me** with CNXyl yielded an imido enamine Ta(V) product. Surprisingly, **1-Cl** reacted with CNXyl (1 equiv.) at the borate backbone of the [H₂B(Mes Im)₂] ligand with concomitant methyl transfer from the metal center to form a new, dianionic scorpionate ligand that supported a Ta(V) dimethyl chloro complex (**6**). Treatment of **1-Cl** with further CNXyl led to an azaallyl scorpionate complex, and an imido isocyanide scorpionate complex, along with propene and xylyl ketenimine. Complex **6** reacted with CO to yield a pinacol scorpionate complex **10** – a new reaction pathway in early transition metal chemistry. Mechanistic studies revealed that this proceeded via migratory

insertion of CO into a Ta-Me group, followed by methyl transfer to form an η^2 -acetone intermediate. Elimination of acetone furnished a CO-stabilized Ta(III) intermediate capable of rebinding and subsequently coupling two equivalents of CO-derived acetone to form the pinacol ligand in 10.

Introduction

One of the most interesting and significant challenges that chemists face today is the clean, efficient utilization of carbon monoxide (CO) as a C₁ source. The foremost example of successful C₁ chemistry is the Fischer-Tropsch process, by which CO and hydrogen gas are combined under high temperature and pressure in the presence of heterogeneous metal catalysts to yield liquid hydrocarbons. Other notable processes that convert feedstock CO into valuable C₁-C_n chemical commodities include the Monsanto² and Cativa³ acetic acid syntheses, as well as hydroformylation, hydrocarboxylation and hydroesterification;⁴ these classic processes are typically mediated by homogeneous late transition metal catalysts. Many of the primary steps in these industrial catalytic processes have been identified by studying the stoichiometric carbonylation chemistry of organometallic complexes.⁵ Undoubtedly, the most studied of these stoichiometric steps is the migratory insertion of CO into metal-alkyl bonds to form a new C-C bond, yielding acyl-containing products.^{6,7} If more than one alkyl group is present on the transition metal center, successive methyl transfers can be observed, yielding products containing more than one new C-C bond.^{8,9} Using this strategy, a wide array of C₂-C_n products can be accessed under mild conditions, including ketones,⁹ enediols,¹⁰⁻¹² enols,^{13,14} alcohols,¹⁰ and ketenes,¹⁵ depending on the number and nature of alkyl groups, the metal center, and reaction conditions that are employed.

While many studies in this area have focused on the stoichiometric reactivity of CO (and the isolobal substrates carbon monosulfide, CS, and isocyanides, CNR) with late transition metal complexes, fewer reports have detailed the fundamental reactivity of CO with early transition metal complexes (here defined as groups 3-6).^{9,16} The extremely oxophilic nature of the early transition metals,¹⁷ along with their high valencies, influences their reactivity with CO and often leads to divergent reactivity relative to that of the later metals.¹⁸ We previously reported the reaction of a β-diketiminate-supported Nb imido dimethyl complex with CO, where a variety of products could be obtained depending on the reaction conditions employed, including acyl-, ketone-, enediol-, and alcohol-containing products.¹⁰ Using this system, we were also able to access a CO-stabilized Nb(III) species (via elimination of CO-derived acetone) that catalyzes alkyne semihydrogenation.¹⁹ Additionally, we reported the carbonylation reaction of a trimethyl Ta complex supported by amidinate ligands, which resulted in the formation of an enediol product; we did not observe reactivity at the third methyl group.¹¹

Taking this chemistry a step further, we sought a group 5 system that would enable us to observe carbonylation reactivity at more than two alkyl groups, as such a strategy could lead to unique products containing multiple equivalents of CO and more than two new C-C bonds. We focused on Ta, as a few prior studies of Ta alkyl systems have demonstrated the ability of more than two methyl groups to react with CO, yielding oligomeric enolate-containing products.^{13,14} These reports invariably use a Cp* (Cp* = pentamethylcyclopentadienyl) ligand to support the Ta metal center. In the present study, we forgo Cp* in favor of a bidentate *N*-heterocyclic carbene (NHC) ligand.^{20,21} While NHC ligands are relatively uncommon in the early transition metal literature,^{22,23} they have been used extensively to support late metal cross-coupling catalysts.²⁴⁻²⁶ Using an NHC ligand, we hypothesized that we could observe coupling of the organic products derived from CO

and methyl groups, as the strong σ -donating and negligible π -back bonding characteristics of these ligands serve to increase electron density at electron-poor early metal centers.²⁷ We recently reported the syntheses of two closely related NHC-supported Ta(V) tri- and tetramethyl complexes $[H_2B(^{Mes}Im)_2]TaMe_3X$ (1-X, X=Cl, Me; Im=imidazole, Im=im

Results and Discussion

Formation of Enolates from Carbon Monoxide and Imines from Xylyl Isocyanide.

Addition of CO (1 atm) to a solution of the tetramethyl bis(NHC)borate Ta(V) precursor **1-Me** resulted in a color change from pale yellow to orange. Upon workup, pale yellow crystals were isolated away from an oily, orange impurity. The X-ray crystal structure revealed uptake of two equivalents of CO to give the oxo enolate methyl Ta(V) compound **2-Me** in 76% yield (Scheme 1, Figure 1). ¹H NMR analysis revealed broad resonances for the protons on the bis(NHC)borate ligand and four sharp, upfield singlets corresponding to chemically inequivalent methyl groups, one attached to the metal center and three decorating the periphery of the CO-derived enolate ligand. Cooling the NMR sample to –10 °C sharpened the resonances of the bis(NHC)borate ligand but did not affect the four upfield methyl signals (Figure S4).

Scheme 1. Syntheses of compounds **2-X** (X = Me, Cl), **3**, **4-X** (X = Me, Cl), and organic product **5**.

Similarly, the trimethyl chloro Ta(V) precursor 1-Cl reacted with two equivalents of CO to form the oxo enolate chloro Ta(V) compound 2-Cl in 64% yield (Scheme 1). Compound 2-Cl also exhibits C₁ symmetry by ¹H NMR, but unlike 2-Me, the signals in the spectrum of 2-Cl are sharp at ambient temperature (Figure S5). Comparison of the crystal structures of compounds 2-Me and 2-Cl (Figure 1) revealed striking similarities: both compounds adopt square-based pyramidal geometries with the oxo ligand in the apical position and have almost identical bond metrics (Table S6). Despite the highly oxophilic nature of Ta,¹⁷ crystallographically characterized examples of Ta complexes with terminal oxo moieties are relatively rare, likely due to the tendency of such complexes to form multinuclear oxo-bridged species.^{29,30} The Ta=O bond lengths observed in 2-X (X = Me, 1.724(3) Å; X = Cl, 1.718(2) Å) are consistent with the data in these few prior reports of Ta-O multiple bonds.^{12,31-36}

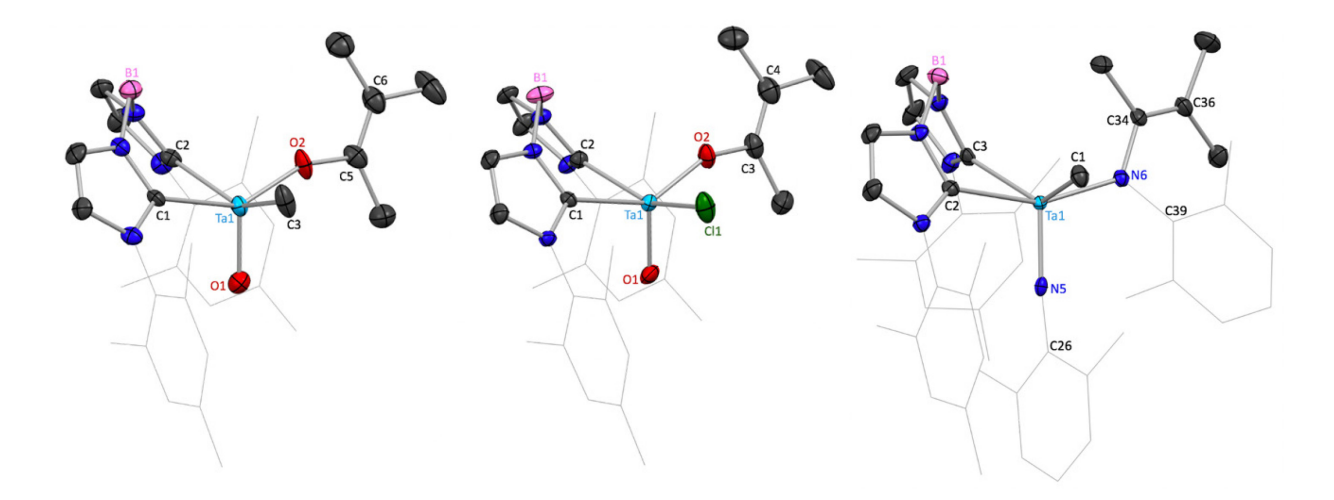


Figure 1. Crystal structures of **2-Me** (left), **2-Cl** (center), and **3** (right) with 50% probability thermal ellipsoids. H atoms are excluded, and mesityl and xylyl groups are depicted in wireframe.

Turning to isocyanides as isolobal analogs of CO, addition of two equivalents of xylyl isocyanide (CNXyl) to a solution of **1-Me** led to formation of an orange-colored product identified as the imido enamine methyl Ta(V) compound **3** in 91% yield (Scheme 1). X-ray diffraction and ¹H NMR studies revealed that the structure of **3** is akin to those of **2-X**, with the imido ligand occupying the apical position of a square-based pyramid (Figure 1). The Ta=N(Xyl) bond length in **3** (1.776(2) Å, Table S7) and the nearly linear Ta=N-C_{Xyl} bond angle (173.34(18)°) are in good agreement with those of previously reported Ta(V) monoimido compounds. ^{35,37-40} Quite surprisingly, compound **1-Cl** did not react in an analogous manner with CNXyl, as detailed below.

Formation of an enolate or enamine moiety from insertion of CO or CNR into early transition metal-methyl bonds is well precedented. In the realm of Ta carbonylation chemistry, Schrock and coworkers first reported this reactivity pattern in 1979: $Ta(\eta^5-Cp^*)Me_4$ reacted with one equivalent of CO to form the η^2 -acetone complex $Ta(\eta^5-Cp^*)(O=CMe_2)Me_2$.¹³ This complex

reacted with a further equivalent of CO to produce a mixture of oxo-bridged oligomeric Ta(V) species containing one enolate ligand per Ta center. Neither the η^2 -acetone complex nor the oligomeric products were crystallographically characterized. A second example of enolate formation from the reaction of CO with Ta-methyl groups was reported in 2008; again, the product, $[TaO(\eta^5-Cp^*)(OSiPh_3)(OC(Me)=C(Me)_2)]_n$, was oligomeric and an X-ray crystal structure was not reported. 14 Thus, complexes 2-X represent the first structurally characterized examples of monomeric Ta enolate complexes formed via this route (although two structurally-characterized Ta bis(enolate) complexes, prepared via salt metatheses between K(OC[Ad]Ar) (Ar = 3,5dimethylphenyl and 2,4,6-trimethylphenyl, Ad = adamantyl) and TaMe₃Cl₂, have been reported).⁴¹ It is likely that the bis(NHC)borate ligand employed in this work offers a greater degree of steric protection than does the Cp* ligand used in these previous studies, thus disfavoring the formation of oligomers. Monomeric Ta enamine complexes formed from the reaction of Ta-alkyl complexes with CNR reagents are more numerous. ^{6,12,14,42-45} In these examples, it is likely that the added steric bulk offered by CNR (relative to CO) disfavors the formation of multinuclear products. The formation of enol or enamine ligands has also been observed following the reactions of various Zr,⁴⁶⁻⁴⁹ Hf,⁴⁷ and W⁵⁰ alkyl complexes with CO or CNR.

The addition of one equivalent of CO to complexes **1-X** led to mixtures of complexes **2-X** and starting material; similarly, the addition of one equivalent of CNXyl to **1-M**e led to a mixture of **3** and starting material. Thus, while we were unable to directly observe the products resulting from the reactions of **1-X** with one equivalent of CO or CNXyl, we propose that our system operates under a mechanism that is consistent with these prior reports (Scheme 2). First, insertion of one equivalent of CY (Y = O or N(Xyl)) into one Ta-Me bond produces η^2 -acyl or η^2 -iminoacyl intermediate **A**. Subsequent methyl transfer furnishes η^2 -acetone or η^2 -imine intermediate **B**. Next,

a second equivalent of CY reacts, either by insertion into the Ta-C bond of the η^2 -acetone/imine moiety to give tantalacyclobutane intermediate **C**, or by insertion into another Ta-Me bond to give η^2 -acetone/imine η^2 -acyl/iminoacyl complex **D**. Finally, C-C coupling and C-Y bond cleavage leads to the isolated products **2-Me**, **2-Cl**, and **3**.

Scheme 2. Proposed mechanism for the formation of compounds **2-X** (X = Cl, Me) and **3** from the reactions of **1-X** (X = Cl, Me) with CY (Y = O, N(Xyl)) reagents.

We next explored the reactivity of complexes 2-X with reagents that could serve as proton or silyl sources, with the anticipation that such reactions could lead to liberation of the enolate ligand as an enol/ketone or silane. Complexes 2-X did not react with weak acids (trialkylammonium salts, 2,6-lutidinium chloride), even upon heating for extended periods. The addition of excess trimethylsilyl chloride to yellow solutions of 2-X led to an immediate reaction, as evidenced by

color changes to darker shades of yellow. ^{1}H NMR analysis revealed formation of the products of 1,2-addition across the Ta-oxo bond, namely the enolate siloxy chloride Ta(V) complexes **4-X**, in 85% (X = Me) and 73% (X=Cl) yield (Scheme 1).

The solid-state structures of **4-Me** and **4-Cl** revealed nearly identical geometries and bond metrics: both complexes adopt distorted octahedral geometries, with the enolate ligand *trans* to a carbene carbon of the bis(NHC)borate ligand (Figure 2, Table S8). The Ta–O(SiMe₃) bonds are lengthened (X=Me, 1.857(2) Å; X = Cl, 1.856(2) Å) relative to the Ta=O bonds in **2-X**. Variable temperature ¹H NMR experiments revealed that compound **4-Me** can adopt two conformations (Figures S11-21). At ambient temperature, the resonances of **4-Me** are broad; upon heating to 40 °C, the signals converge into a single set of sharp peaks. Cooling to –70 °C resulted in resolution of the signals into two equivalent sets of sharp resonances. We suggest that the two conformational isomers are differentiated by the identity of the ligand (either Me or Cl) *trans* to the siloxy group, leading to the observed fluxional behavior.

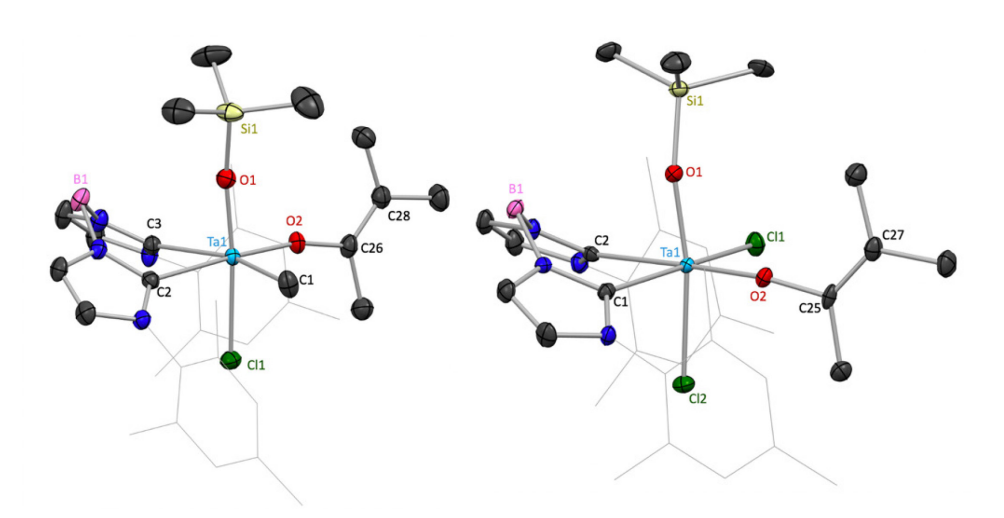


Figure 2. Crystal structures of **4-Me** (left) and **4-Cl** (right) with 50% probability thermal ellipsoids. H atoms are excluded, and mesityl groups are depicted in wireframe.

Formation of compounds **4-X** serves as a rare example of 1,2-addition across a Ta-O multiple bond. A similar complex, $[Ta(OSiMe_3)Cl(\eta^5-Cp^*)(\eta^5-C_5H_4SiMe_3)][F_3CSO_3]$, was synthesized from the reaction of $Ta(=O)Cl(\eta^5-Cp^*)(\eta^5-C_5H_4SiMe_3)$ with $F_3CSO_3SiMe_3$. However, in this case the trimethylsilyl group merely served to cap the oxo ligand and generate a cationic Ta(V) siloxy complex. Indeed, while there have been a handful of reports of 1,2-addition across highly polarized, group 4 metal-oxo bonds, $^{51-53}$ examples of such reactivity in group 5 metal complexes are uncommon. We recently reported an oxo imido Nb(V) complex that was capable of adding secondary and tertiary silanes across the Nb=O bond, 54 where we employed a π -loading 55 strategy specifically to enhance the reactivity of the oxo ligand. In the present work, it is likely that capping the Ta=O moieties of **2-X** with a silyl group serves to remove electron density from the already electron-rich Ta center, which is supported by several strongly electron-donating groups (i.e. the bis(NHC)borate, oxo, and enolate ligands). Thus, while we were unable to release the enolate ligands of **2-X** by reactions with weak acids, we were able to observe atypical reactivity across a group 5 metal-oxo group.

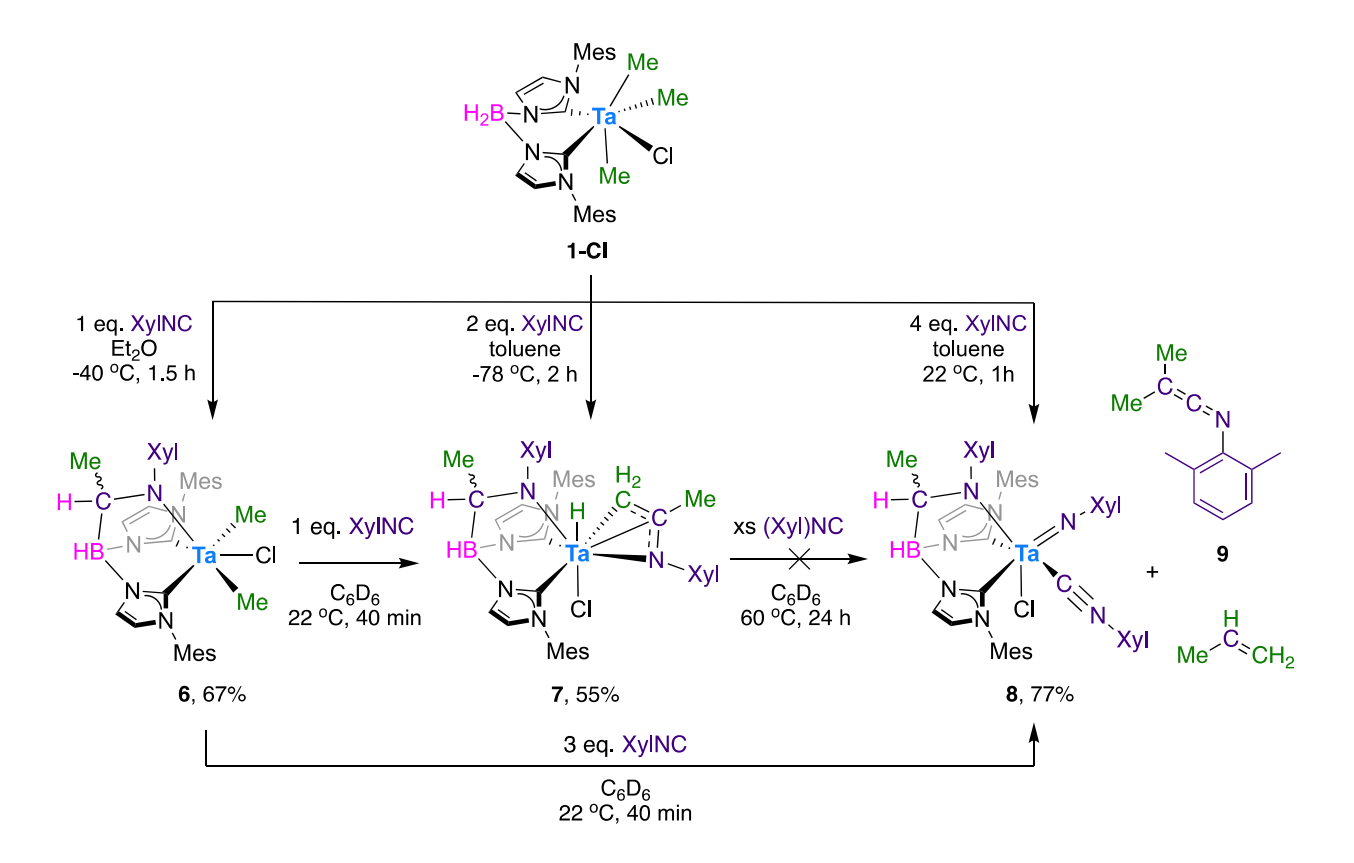
In contrast, the enamine ligand in 3 could be protonated to give the corresponding free imine. Addition of two equivalents of lutidinium chloride to a solution of 3 in C_6D_6 and subsequent sonication resulted in a heterogeneous mixture with tan solids. Analysis of the solution by 1H NMR revealed complete and clean conversion to the free imine, N-(1,2-dimethylpropylidene)-2,6-dimethylbenzenamine (5) and lutidine (Scheme 1). A 20:1 ratio of E:Z isomers of 5 could be observed in the 1H NMR spectrum (Figure S25). No tantalum species could be observed by NMR, suggesting that the insoluble tan precipitate contains a mixture of insoluble Ta-oxo species. Mass

spectrometry analysis of the pale orange solution further confirmed the presence of imine 5 (m/z: 189).

Formation of Xylyl Ketenimine and Propene from Xylyl Isocyanide.

Addition of one equivalent of CNXyl to 1-Cl at -40 °C resulted in an immediate color change from yellow to yellow-orange. After stirring the resulting mixture at -10 °C for 1.5 h and subsequent workup, yellow microcrystals were obtained. NMR analysis revealed several diagnostic resonances, indicating formation of the dimethyl chloro scorpionate Ta(V) complex 6 in 67% yield (Scheme 3). In the ¹H NMR spectrum, the broad signal corresponding to the protons on the borate group integrated to one, rather than two protons, and was now accompanied by a quartet integrating to one proton (Figure S27). In addition, only two resonances for Ta-methyl groups could be identified in the spectrum, and a new doublet integrating to three protons appeared upfield. In the ¹¹B NMR spectrum, a single broad resonance at –0.35 ppm could be assigned to the borate group (Figure S29); in contrast, this signal appears between -8.11 and -2.82 ppm in the spectra of complexes 2-X, 3, and 4-X. Taken together, these data suggested that complex 1-Cl had reacted at the borate group of the bis(NHC)borate ligand to produce a dianionic C,N,C-scorpionate ligand⁵⁶ comprised of two neutral NHCs and one negatively charged amido group, all linked via an anionic borate group. The scorpionate ligand likely formed following migratory insertion of CNXyl into a Ta-Me bond to give a [MeCNXyl] group, which subsequently inserted into a B-H bond of the bis(NHC)borate ligand.

Scheme 3. Syntheses of compounds 6, 7, 8, and organic side products 9 and propene from 1-Cl. Compounds 7, 8, and 9 can also be synthesized from compound 6.



X-ray crystallographic analysis (Figure 3) showed that the Ta center in 6 lies in a distorted octahedral geometry, with the donor atoms of the scorpionate ligand making up one face of an octahedron and the two methyl groups and chloro ligand making up another face. Notably, the scorpionate ligand is chiral: the transfer of a methyl group to the carbon atom linking the amido nitrogen to the boron atom results in the formation of a stereocenter. In the solid-state structure, we observed positional disorder at the xylylamido moiety, including the chiral center and the attached methyl group. Modeling the two positions for the stereocenter as either the *R*- or *S*-enantiomer resulted in a stable structure solution with each part in roughly 50% occupancy, implying that the *R*- and *S*-enantiomers are present in a ca. 1:1 ratio in the solid-state structure.

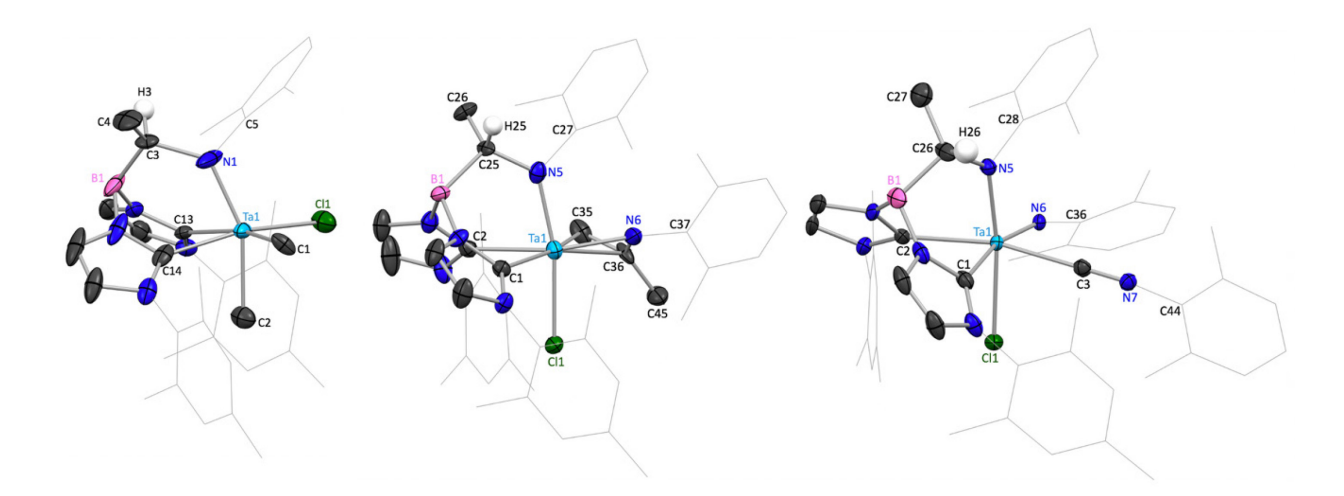


Figure 3. Crystal structures of **6** (left), **7** (center), and **8** (right) with 50% probability thermal ellipsoids. H atoms (except the hydrogen on the chiral center of the scorpionate ligand), disordered fragments of the molecules (**6** and **7**) and lattice solvent (**8**) are excluded, and mesityl and xylyl groups are depicted in wireframe. A Q peak corresponding to the tantalum hydride in **7** could not be located in the Fourier difference map.

We have previously reported chemically noninnocent behavior at the borate group of this bis(NHC)borate ligand: reaction of [H₂B(^{Mes}Im)₂]Nb(N'Bu)Me₂ with excess CO resulted in the formation of a transient η²-acetone product that subsequently released an equivalent of acetone.²¹ The liberated acetone inserted into the B-H bond of the bis(NHC)borate ligand to generate a monoanionic, tridentate boryl isopropoxide ligand, which ligated a CO-stabilized Nb(III) metal center. This mode of hydroboration reactivity was also observed to occur with ketones, aldehydes, and isocyanates, and in some cases double insertion into both B-H bonds was observed. The present work differs from this previous report in that the newly formed tridentate ligand is dianionic, rather than monoanionic.

Complex 1-Cl was observed to react with further equivalents of CNXyl: addition of two equivalents of CNXyl to a yellow solution of 1-Cl at -78 °C resulted in an immediate color change to dark orange. After stirring this mixture at -78 °C for two hours and subsequent workup, dark orange crystals were obtained. ¹H NMR analysis revealed formation of the hydrido chloro azaallyl Ta(V) complex 7 in 55% yield, ligated by the aforementioned dianionic scorpionate ligand (Scheme 3). The azaallyl group was likely formed via insertion of CNXyl into a Ta-Me bond, followed by migration of a second Ta-Me group to give a transient η^2 -imine complex; subsequent β-hydride elimination at one of the imine methyl groups furnished the final product. In the ¹H NMR spectrum, a resonance at 17.34 ppm integrating to one proton could be assigned to the metal hydride (Figure S30). Interestingly, this resonance is split into a doublet (${}^{3}J = 3.3 \text{ Hz}$) instead of the expected singlet due to three-bond coupling to one of the methylene protons of the azaallyl moiety. Off-diagonal cross peaks between the Ta-H peak and the methylene proton resonance were observed in a ¹H-¹H COSY NMR spectrum of 7, further confirming three-bond coupling between these two protons (Figure S34). Additionally, the two methylene proton resonances appear at distinct chemical shifts: a doublet at 3.02 ppm ($^{3}J = 3.3$ Hz) and a singlet at 3.94 ppm, both integrating to one proton. Cross-peaks between these proton signals and the methylene carbon resonance were observed in a ¹H-¹³C HSQC NMR spectrum of 7 (Figure S33).

In the solid-state structure, the azaallyl ligand in 7 is in the same plane as the NHC groups of the scorpionate ligand, while the chloro ligand is *trans* to the scorpionate amido group (Figure 3). Positional disorder of the azaallyl group and the scorpionate amido moiety prevented us from locating a Q peak corresponding to the Ta hydride. While we were unable to crystallographically confirm the presence of a metal hydride, the NMR data for this compound strongly supports our assignment, as discussed above. The disorder at the chiral carbon of the scorpionate amido group

in 7 is identical to the disorder described above for 6: modeling the two positions for the stereocenter as either the *R*- or *S*-enantiomer resulted in a stable structure solution with each part in roughly 50% occupancy.

Complex 7 could be cleanly generated in C_6D_6 solution by the addition of one equivalent of CNXyl to 6 (Scheme 3). This suggests that 6 is an intermediate along the path to 7. Further, it can be concluded that formation of the scorpionate ligand likely occurs first, followed by reaction of a second equivalent at the Ta-Me groups to generate an η^2 -imine moiety, which subsequently undergoes β -hydride elimination to yield the azaallyl ligand. Similar β -hydride elimination of an η^2 -imine bound to a Ta center was observed following the reaction of $(\eta^2-C_2B_9H_{11})$ TaMe₃ with CNAd (Ad = adamantyl).⁵⁸

Reactions of 1-CI with further equivalents of CNXyl all led to a third scorpionate product, the imido chloro isocyanide scorpionate Ta(V) complex **8**, with the use of four equivalents resulting in the cleanest reaction and highest yield (77%, Scheme 3). The room temperature ¹H NMR spectrum of the dark orange product appeared to indicate the presence three similar compounds, based on the presence of three quartets between 3.5-4.2 ppm, corresponding to the proton on the chiral carbon of the scorpionate ligand (Figure S35). Repeated recrystallizations did not affect the relative magnitude of these signals, which were present in a ca. 2:1:2 ratio. A variable temperature ¹H NMR experiment provided clarity: upon heating to 100 °C, the ¹H NMR spectrum simplified dramatically and only one quartet remained at 3.70 ppm, suggesting that we were observing a mixture of isomers that interconvert on the NMR timescale at elevated temperatures (Figures S38-43; see p. S23 for a detailed discussion of isomerism in complex **8**). The three sets of resonances observed at ambient temperature resolved into two sets of peaks upon cooling to -45 °C. In the

FT-IR spectrum, we observed a strong absorbance at 2180 cm⁻¹ that we attributed to a CNXyl C≡N stretch (Figure S84).

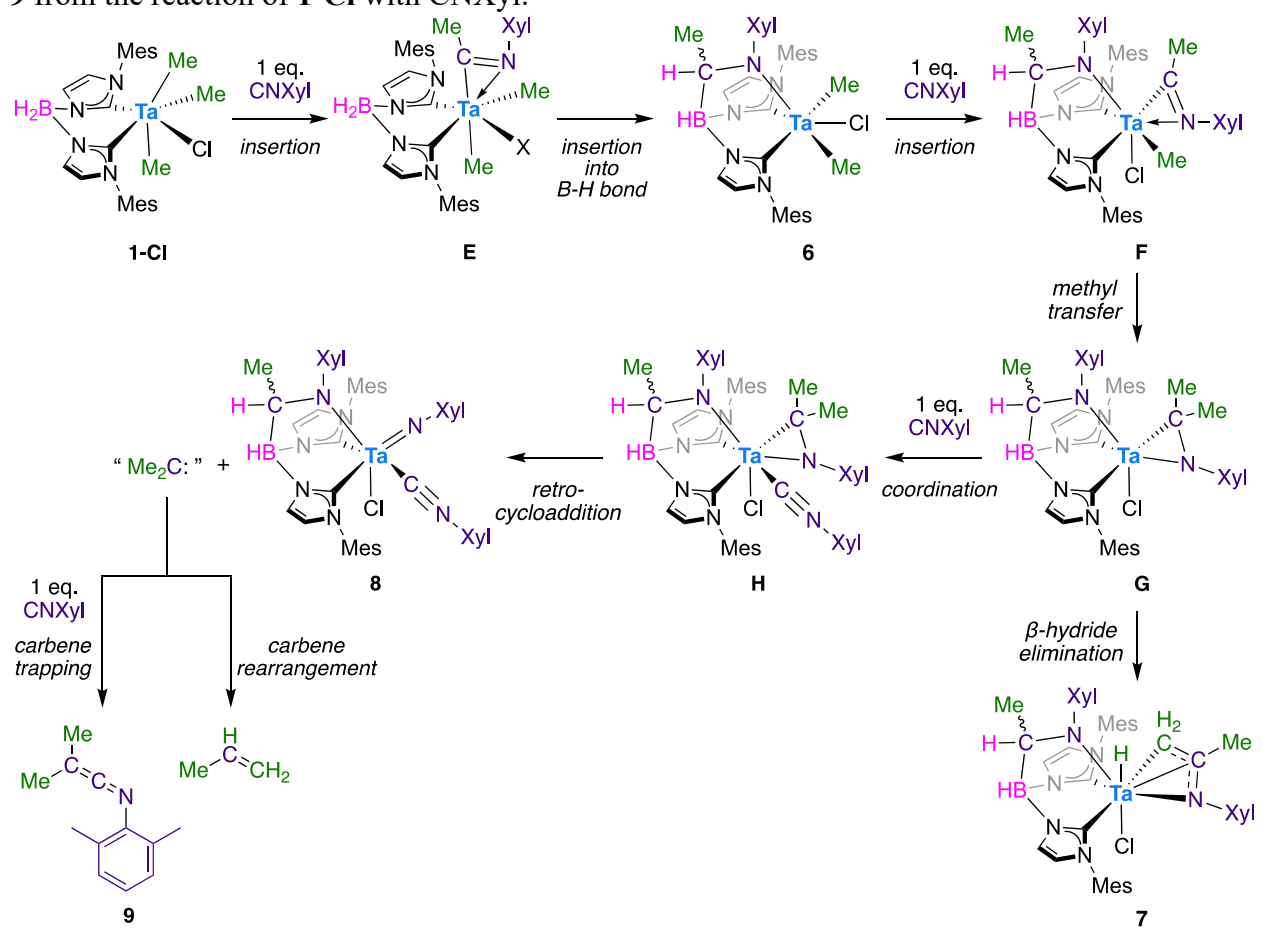
Unlike compounds **6** and **7**, the solid-state structure of **8** exhibited no disorder at the chiral amido moiety (Figure 3). The Ta=N(Xyl) bond is lengthened (1.823(2)Å, Table S11) and the Ta=N-C_{Xyl} bond angle is more bent (161.32(19)°) in complex **8** than was observed in imido enamine complex **3**. The metal center sits in a distorted octahedral environment, with the imido and isocyanide groups in the same plane as the NHC groups of the scorpionate ligand and the chloro ligand *trans* to the amido nitrogen.

Complex **8** was cleanly generated in C_6D_6 solution by addition of two or three equivalents of CNXyl to **6** (Scheme 3). As with **7**, this result suggests that **6** is an intermediate along the path to **8**. Generation of **8** in solution, from either **6** or **1-Cl**, enabled us to observe the organic side products generated in these reactions: propene and dimethyl xylyl ketenimine (**9**, Me₂C=C=NXyl, Scheme 3). Reaction of **1-Cl** with four equivalents of CNXyl resulted in the clean formation of **8** and ketenimine **9** (Figure S46). Mass spectrometry analysis of this reaction mixture further confirmed the presence of **9** (m/z: 173). Reaction of **6** with two equivalents of CNXyl led to formation of **8**, ketenimine **9**, and trace amounts of propene, as observed in the ¹H NMR spectrum (Figure S45); carrying out the same reaction with three equivalents of CNXyl led only to the formation of **8** and **9**. Complex **8** could not be generated from azaallyl hydrido complex **7**, suggesting that β -hydride elimination at the η^2 -imine moiety is irreversible.

Taken together, these NMR observations allow us to piece together a possible mechanism for the formation of **8**, as depicted in Scheme 4. Combination of **1-Cl** with CNXyl first leads to formation of iminoacyl intermediate **E** via migratory insertion. The newly formed [MeCNXyl] group then inserts into a B-H bond to form scorpionate complex **6**. Then, a second equivalent of

CNXyl inserts to form iminoacyl intermediate \mathbf{F} , which subsequently undergoes methyl group transfer to form transient η^2 -imine complex \mathbf{G} . In the absence of additional equivalents of CNXyl, the η^2 -imine moiety undergoes beta hydride elimination to form 7. In the presence of additional CNXyl, η^2 -imine complex \mathbf{G} continues reacting: a third equivalent of CNXyl binds to the metal center to give η^2 -imine isocyanide intermediate \mathbf{H} . This binding event provides the impetus for cleavage of the η^2 -imine C-N bond to give $\mathbf{8}$ and a dimethylcarbene fragment, which can be trapped by CNXyl to give ketenimine $\mathbf{9}$ or, in absence of a fourth equivalent of CNXyl, rearrange to give propene.

Scheme 4. Proposed mechanism for the formation of complexes 6, 7, 8, propene, and ketenimine 9 from the reaction of 1-Cl with CNXyl.



Two similar examples of ketenimine formation from Ta-Me groups and CNR reagents have been reported. First, reaction of Ta(η^5 -Cp*)Me₂Cl₂ with CNXyl or CNMes led to formation of Ta-imido products and the corresponding ketenimines Me₂C=C=NXyl and Me₂C=C=NMes.⁴⁴ A second report detailed formation of Me₂C=C=NDipp (Dipp = 2,6-diisopropylphenyl), which was generated following reaction of [η^1 : η^5 -(Me₂NCH₂CH₂)C₂B₉H₁₀]TaMe₃ with three equivalents of CNDipp.⁵⁹ The related reaction of [η^1 : η^5 -(Me₂NCH₂CH₂)C₂B₉H₁₀]TaMe₃ with one or two equivalents of the less sterically encumbering CNXyl also led to the formation of a dimethylcarbene fragment, but in this case the carbene inserted into a B-H bond of the carborane cage.

Formation of Pinacol from Carbon Monoxide or Acetone.

Addition of CO (1 atm) to a solution of **6** resulted in successive color changes from yellow to dark yellow to orange. Small amounts of yellow microcrystals were isolated from the reaction mixture; 1 H NMR analysis revealed formation of a new product that retained the dianionic scorpionate ligand and possessed *four* chemically inequivalent methyl groups (Figure S47). Reaction of **6** with 13 C-enriched CO (99% 13 C) yielded a similar product that displayed two intense doublets with J = 35.4 Hz in the 100-107 ppm region of the 13 C{ 1 H} NMR spectrum, which suggested a bond between two chemically distinct but strongly coupled 13 C atoms (Figure S52). These data revealed formation of the pinacol scorpionate Ta(V) complex **10** (Scheme 5). Two equivalents of dimethyl starting material are required to form one equivalent of **10**, which was isolated in poor yield via this route (**10**, 31%; **10**-*C,*C, 27%). Interestingly, in the 1 H NMR spectrum of the 13 CO-labeled product **10**-*C,*C, the four pinacol methyl resonances are split into

virtual triplets with ${}^2J = 3.6$ Hz due to two-bond coupling with a 13 C atom that is strongly coupled to the other 13 C atom, producing four signals with AA'X₃ splitting patterns (Figures S50-51). The 1 H-coupled 13 C NMR spectrum exhibited further splitting of the pinacol carbon doublets into broad triplets with ${}^{2}J = 3.0$ Hz (Figure S53).

Scheme 5. Synthesis of compounds **10** and **10-***C,*C from the reactions of **6** with CO and ¹³CO, respectively (top). Synthesis of compounds **10**, **10-** d_{12} , and **11** from the reaction of **6** with H₂ and excess ketone (bottom).

$$\begin{array}{c} \text{Me} \\ \text{Me} \\ \text{Me} \\ \text{Me} \\ \text{HB} \\ \text{N} \\ \text{Me} \\$$

The solid-state structure of **10** exhibited a distorted octahedral geometry about the metal center, with the chloro ligand *trans* to the amido nitrogen and the pinacol ligand bound in the same plane as the two NHC groups (Figure 4). Complex **10** crystallized in an orthorhombic space group (*Pnma*), with half of the molecule present in the asymmetric unit (a vertical mirror plane bisects the pinacol ligand). In this case, the chiral carbon of the scorpionate ligand was not positionally disordered, but the methyl group and proton bound to it were. Modeling the methyl and proton moieties as either the *R*- or *S*-configuration in 50% occupancy led to a stable structure solution.

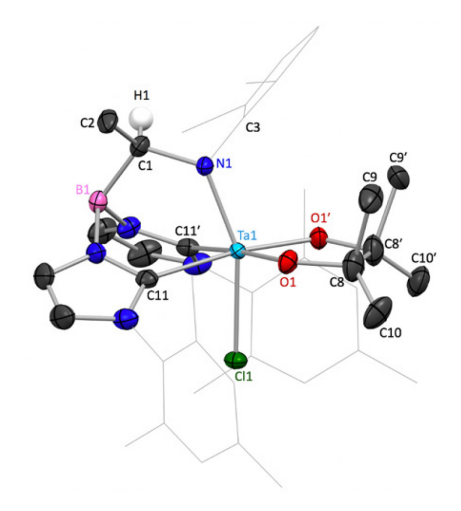


Figure 4. Crystal structure of **10** with 50% probability thermal ellipsoids. H atoms (except the hydrogen on the chiral center of the scorpionate ligand) and disordered fragments of the molecule are excluded, and mesityl and xylyl groups are depicted in wireframe.

To our knowledge, formation of a pinacol ligand from metal-bound methyl groups and CO is unprecedented. To learn more about the mechanism of this transformation, we monitored the reaction of **6** with 13 CO by 13 C{ 1 H} NMR spectroscopy (Figure 5 and Figures S54-57). After 10 min, two intense singlets appeared at 161.79 and 161.82 ppm, which were assigned as η^{2} -acyl intermediates; we suggest that the asymmetry of the chiral ligand leads to two chemically distinct binding orientations for the acyl group, leading to the appearance two singlets for two stereoisomers. After 1 h, a resonance appeared at 184.5 ppm, corresponding to free 13 CO, as well as two doublets at 106.4 and 100.3 ppm for the 13 C atoms of product **10**. In addition, two singlets appeared at 102.4 and 102.76 ppm, likely corresponding to two closely related η^{2} -acetone complexes. Schrock and coworkers report the 13 C shift for a similar η^{2} -acetone complex, Cp*TaMe₂(η^{2} -acetone), at 111 ppm. 13 Finally, four singlets at 262.2, 260.0, 231.05, and 230.97

ppm appeared to grow in and disappear at the same rate. The resonances at 262.2 and 260.0 ppm likely correspond to Ta-bound 13 CO; the CO carbon resonance in a related complex, [BDI]Nb(N^tBu)(CO)₂, appears at 255.6 ppm. 10 The remaining two singlets at 231.05, and 230.97 ppm could correspond to carbonyl carbons of two stereoisomeric η^1 -acetone complexes. The carbonyl carbon 13 C resonance in early transition metal η^1 -acetone complexes typically appears in the 204.3-226.6 ppm range. $^{60\text{-}62}$ Taken together, we suggest that these four singlets correspond to a CO-stabilized Ta(III) η^1 -acetone intermediate. As time progressed, the η^2 -acyl, η^2 -acetone, and η^1 -acetone intermediates grew in and then disappeared as the amount of 10 increased. Free 13 C-labeled acetone was not observed in any of the spectra.

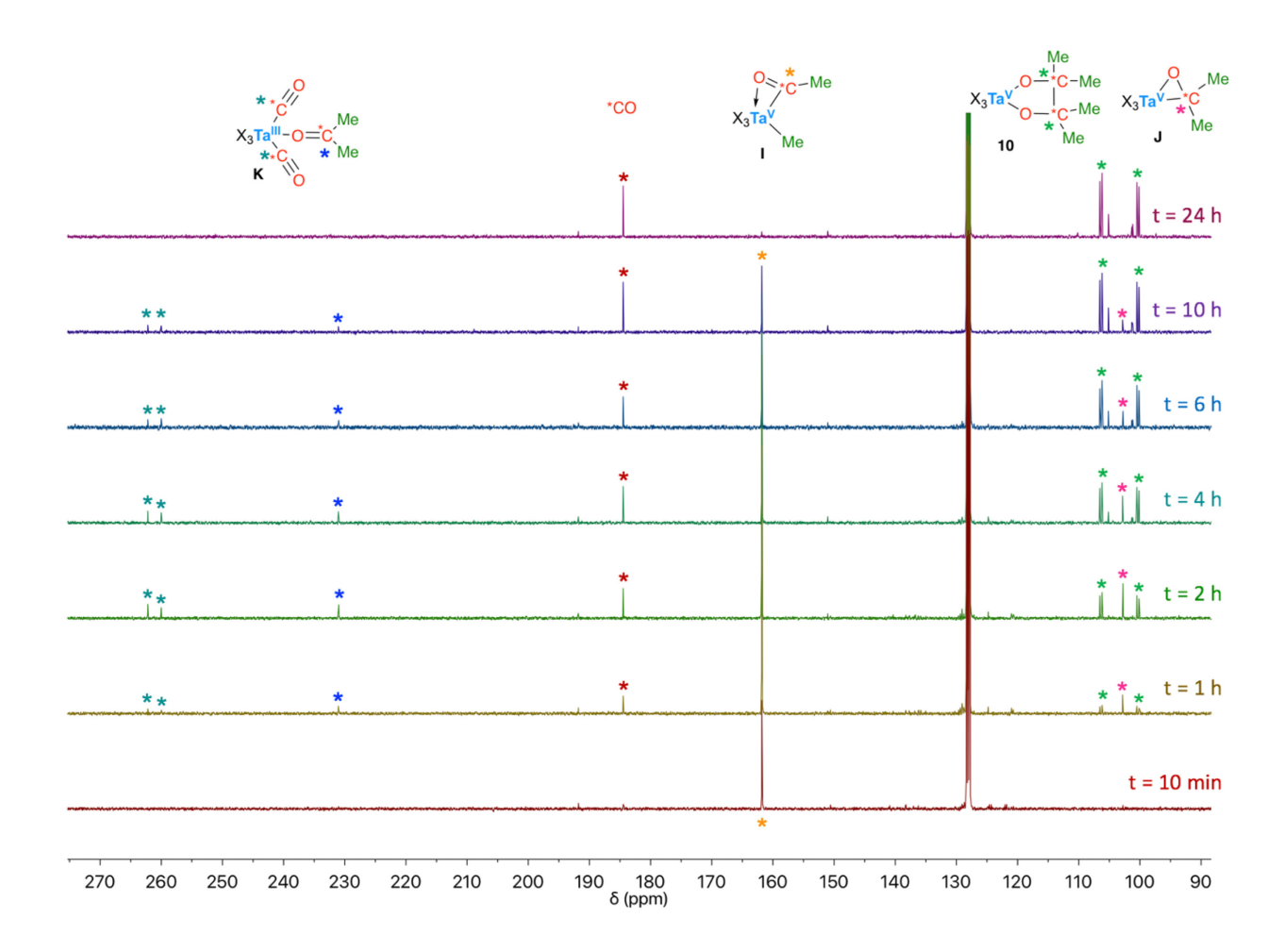


Figure 5. 13 C $\{^{1}$ H $\}$ NMR spectra of the reaction of 6 with 13 CO to give 10 (298 K, 101 MHz, C₆D₆).

Based on these NMR data, we propose that reaction of 6 with CO could follow the mechanism outlined in Scheme 6. First, migratory insertion of CO into a Ta-Me group gives η^2 -acyl intermediate **I**; transfer of a second methyl group furnishes η^2 -acetone intermediate **J**. Isomerization of η^2 -acetone to η^1 -acetone yields low valent Ta(III) intermediate **K**, which is stabilized by π -back bonding interactions with CO ligands (path 1). Intermediate **K** can eliminate acetone to furnish transient Ta(III) intermediate **L** (not observed in the ¹³C NMR monitoring experiment), which is unstable and either re-binds acetone or reacts deleteriously to form unidentified side products. The newly generated free equivalent of acetone quickly reacts with η^2 -acetone intermediate **J** via insertion of the carbonyl into the Ta-C bond, yielding complex **10** (path 2).

Scheme 6. Proposed mechanism for the formation of pinacol complex **10** from dimethyl complex **6** and CO-derived acetone.

$$X_{3}Ta^{V} = \begin{bmatrix} 1 & \text{eq.} & \text{Oolemotion} \\ \text{Me} & \text{Insertion} \end{bmatrix} \begin{bmatrix} \text{Ne} & \text{Ta reduction} \\ \text{Me} & \text{Ta oxidation} \end{bmatrix} \begin{bmatrix} \text{Me} & \text{Ta oxidation} \\ \text{Me} & \text{Ta oxidation} \end{bmatrix} \begin{bmatrix} \text{Me} & \text{Me} \\ \text{Me} & \text{Me} \end{bmatrix} \begin{bmatrix} \text{Me} & \text{Me} \\ \text{Me} & \text{Me} \end{bmatrix} \begin{bmatrix} \text{Me} & \text{Me} \\ \text{Me} & \text{Me} \end{bmatrix} \begin{bmatrix} \text{Me} & \text{Me} \\ \text{Me} & \text{Me} \end{bmatrix} \begin{bmatrix} \text{Me} & \text{Me} \\ \text{Me} & \text{Me} \end{bmatrix} \begin{bmatrix} \text{Me} & \text{Me} \\ \text{Me} & \text{Me} \end{bmatrix} \begin{bmatrix} \text{Me} & \text{Me} \\ \text{Me} & \text{Me} \end{bmatrix} \begin{bmatrix} \text{Me} & \text{Me} \\ \text{Me} & \text{Me} \end{bmatrix} \begin{bmatrix} \text{Me} & \text{Me} \\ \text{Me} & \text{Me} \end{bmatrix} \begin{bmatrix} \text{Me} & \text{Me} \\ \text{Me} & \text{Me} \end{bmatrix} \begin{bmatrix} \text{Me} & \text{Me} \\ \text{Me} & \text{Me} \end{bmatrix} \begin{bmatrix} \text{Me} & \text{Me} \\ \text{Me} & \text{Me} \end{bmatrix} \begin{bmatrix} \text{Me} & \text{Me} \\ \text{Me} & \text{Me} \end{bmatrix} \begin{bmatrix} \text{Me} & \text{Me} \\ \text{Me} & \text{Me} \end{bmatrix} \begin{bmatrix} \text{Me} & \text{Me} \\ \text{Me} & \text{Me} \end{bmatrix} \begin{bmatrix} \text{Me} & \text{Me} \\ \text{Me} & \text{Me} \end{bmatrix} \begin{bmatrix} \text{Me} & \text{Me} \\ \text{Me} & \text{Me} \end{bmatrix} \begin{bmatrix} \text{Me} & \text{Me} \\ \text{Me} & \text{Me} \end{bmatrix} \begin{bmatrix} \text{Me} & \text{Me} \\ \text{Me} & \text{Me} \end{bmatrix} \begin{bmatrix} \text{Me} & \text{Me} \\ \text{Me} & \text{Me} \end{bmatrix} \begin{bmatrix} \text{Me} & \text{Me} \\ \text{Me} & \text{Me} \end{bmatrix} \begin{bmatrix} \text{Me} & \text{Me} \\ \text{Me} & \text{Me} \end{bmatrix} \begin{bmatrix} \text{Me} & \text{Me} \\ \text{Me} & \text{Me} \end{bmatrix} \begin{bmatrix} \text{Me} & \text{Me} \\ \text{Me} & \text{Me} \end{bmatrix} \begin{bmatrix} \text{Me} & \text{Me} \\ \text{Me} & \text{Me} \end{bmatrix} \begin{bmatrix} \text{Me} & \text{Me} \\ \text{Me} & \text{Me} \end{bmatrix} \begin{bmatrix} \text{Me} & \text{Me} \\ \text{Me} & \text{Me} \end{bmatrix} \begin{bmatrix} \text{Me} & \text{Me} \\ \text{Me} & \text{Me} \end{bmatrix} \begin{bmatrix} \text{Me} & \text{Me} \\ \text{Me} & \text{Me} \end{bmatrix} \begin{bmatrix} \text{Me} & \text{Me} \\ \text{Me} & \text{Me} \end{bmatrix} \begin{bmatrix} \text{Me} & \text{Me} \\ \text{Me} & \text{Me} \end{bmatrix} \begin{bmatrix} \text{Me} & \text{Me} \\ \text{Me} & \text{Me} \end{bmatrix} \begin{bmatrix} \text{Me} & \text{Me} \\ \text{Me} & \text{Me} \end{bmatrix} \begin{bmatrix} \text{Me} & \text{Me} \\ \text{Me} & \text{Me} \end{bmatrix} \begin{bmatrix} \text{Me} & \text{Me} \\ \text{Me} & \text{Me} \end{bmatrix} \begin{bmatrix} \text{Me} & \text{Me} \\ \text{Me} & \text{Me} \end{bmatrix} \begin{bmatrix} \text{Me} & \text{Me} \\ \text{Me} & \text{Me} \end{bmatrix} \begin{bmatrix} \text{Me} & \text{Me} \\ \text{Me} & \text{Me} \end{bmatrix} \begin{bmatrix} \text{Me} & \text{Me} \\ \text{Me} & \text{Me} \end{bmatrix} \begin{bmatrix} \text{Me} & \text{Me} \\ \text{Me} & \text{Me} \end{bmatrix} \begin{bmatrix} \text{Me} & \text{Me} \\ \text{Me} & \text{Me} \end{bmatrix} \begin{bmatrix} \text{Me} & \text{Me} \\ \text{Me} & \text{Me} \end{bmatrix} \begin{bmatrix} \text{Me} & \text{Me} \\ \text{Me} & \text{Me} \end{bmatrix} \begin{bmatrix} \text{Me} & \text{Me} \\ \text{Me} & \text{Me} \end{bmatrix} \begin{bmatrix} \text{Me} & \text{Me} \\ \text{Me} & \text{Me} \end{bmatrix} \begin{bmatrix} \text{Me} & \text{Me} \\ \text{Me} & \text{Me} \end{bmatrix} \begin{bmatrix} \text{Me} & \text{Me} \\ \text{Me} & \text{Me} \end{bmatrix} \begin{bmatrix} \text{Me} & \text{Me} \\ \text{Me} & \text{Me} \end{bmatrix} \begin{bmatrix} \text{Me} & \text{Me} \\ \text{Me} & \text{Me} \end{bmatrix} \begin{bmatrix} \text{Me} & \text{Me} \\ \text{Me} & \text{Me} \end{bmatrix} \begin{bmatrix} \text{Me} & \text{Me} \\ \text{Me} & \text{Me} \end{bmatrix} \begin{bmatrix} \text{Me} & \text{Me} \\ \text{Me} & \text{Me} \end{bmatrix} \begin{bmatrix} \text{Me} & \text{Me} \\ \text{Me$$

Several prior reports support our mechanistic proposal. Reports of acetone formation from reaction of metal-methyl groups with CO are legion: examples of such reactivity can be found for most of the early- to mid-transition metals, including Ti, ⁶³ Zr, ^{64,65} V, ⁶⁶ Nb, ^{10,19,21,67} Ta, ^{12-14,68} W, ⁵⁰ and Re. ⁶⁹ In these examples, the newly formed acetone either remains bound to the metal center as an η²-acetone ligand or dissociates to give a low valent metal center and free acetone. Additionally, there are several noteworthy examples of low valent and masked low valent early transition metal complexes reductively coupling ketones to give diol ligands (relevant examples: Ti, ^{70,71} Zr, ⁶⁴ V, ⁷² Nb, ^{29,73} Ta, ⁷⁴ Mo, ⁷⁵ and W⁷⁶), with the most famous being the low valent Ti-catalyzed McMurry reaction. ⁷⁷ Two mechanistic proposals are generally invoked in these ketone-coupling reports: the dimerization of ketyl radicals (radical mechanism) or carbonyl insertion into the M-C bond of an η²-acetone intermediate (non-radical mechanism). The Ti-catalyzed McMurry reaction was originally thought to proceed via the radical mechanism; however, a computational study carried out years later provided support for the nonradical mechanism. ⁷⁸ The nonradical

mechanism is also supported by several reports of isolated η^2 -ketone complexes reacting with ketones to yield diol products. 64,75,76

To test if a radical pathway could be operative in our system, we carried out the reaction of 6 with CO in the presence of excess 9,10-dihydroanthracene, a radical scavenger. This reaction resulted in relatively clean conversion to 10, suggesting either that radicals were not formed along the reaction pathway, or that the trap was not potent enough to intercept them (Figure S58). To provide further experimental insight into our proposed mechanism, we carried out isotope labeling studies with acetone-d₆. Reaction of 6 with CO and 0.5 equivalents of acetone-d₆ in C₆D₆ led to formation of isotopologues 10, $10-d_6$, and $10-d_{12}$, the products of coupling two equivalents of proteo-acetone, one equivalent of each proteo- and deutero-acetone, and two equivalents of deutero-acetone, respectively (Scheme 7). Conveniently, the signals for the pinacol methyl groups in the ¹H NMR spectra of **10** and **10-d₆** appear at slightly different chemical shifts, enabling rough quantification of the relative amounts of these products by integration (Figures S59-63, S73 and p. S31). Compounds 10, 10- d_6 , and 10- d_{12} were formed in an approximately 1:4:1 ratio, with minimal generation of side products, as evidenced by ¹H NMR spectroscopy. Since proteo- and deutero-acetone are present in an equimolar ratio in the reaction mixture, a 1:2:1 statistical distribution of these products is expected (assuming a negligible secondary kinetic isotope effect); the greater-than-expected amount of mixed proteo/deutero product 10- d_6 suggests reaction of η^2 acetone intermediate J with free acetone (path 2) is faster than Ta reduction and acetone elimination (path 1). Notably, formation of 10-d₁₂ suggests that both steps of path 1 are reversible, as CO-generated proteo acetone must be exchanged for deutero acetone in order to form deuterated product **10-***d*₁₂.

Scheme 7. Synthesis of a ca. 1:4:1 mixture of complexes 10, $10-d_6$, and $10-d_{12}$ from the reaction of 6 with CO and acetone- d_6 .

Me
$$XyI$$
 Mes I Me I Mes I Mes

To ensure the validity of the labeling experiment, **10-***d*₁₂ was independently synthesized and combined with an equimolar amount of **10** in C₆D₆, and the mixture was subsequently monitored for isotopic scrambling by ¹H NMR spectroscopy. Formation of **10-***d*₆ or scrambling of deuterium into other positions of the molecule were not observed, even upon heating for several days; this suggests that pinacol formation is irreversible under these conditions (Figures S67-68). Complex **10** was stable to heating under an atmosphere of H₂, and the pinacol ligand could not be liberated by silylation with trimethylsilyl reagents. Addition of lutidinium chloride to a solution of **10** led to an intractable mixture of products, as evidenced by ¹H NMR spectroscopy, with no evidence of pinacol in the NMR spectrum. Additionally, solutions of **10** in acetone decomposed over the course of 24 h to yield intractable mixtures of products in the ¹H NMR spectrum. Similarly-concentrated

solutions of 10 in acetone- d_6 decomposed more slowly (4 days), suggesting that C-H (or C-D) activation of acetone leads to decomposition of the product.

Interestingly, 10 could also be accessed via a second route: reaction of 6 with H₂ in excess acetone resulted in formation of 10 in much higher yield (64%; Scheme 5) with a shorter reaction time (12 h) than the corresponding reaction with CO (31%; 48 h). The deuterated product, 10-d₁₂, was also synthesized via this route upon replacing acetone with acetone- d_6 (60% yield, Scheme 5). Additionally, the 3-pentanone coupling product 11 could be generated in 64% yield (Scheme 5), but this reductive coupling methodology could not be extended to benzophenone or benzaldehyde. As outlined in Scheme 8, we suggest that the reaction of 6 with H₂ and ketones follows a pathway similar to that of the corresponding reaction with CO. First, reaction of 6 with H₂ likely generates the transient low valent Ta(III) intermediate **O**, through a series of reductive eliminations from the putative dihydride and/or hydride intermediates ${\bf M}$ and ${\bf N}.^{28,79-81}$ Low valent intermediate O proceeds to reductively bind one equivalent of ketone to form η^2 -ketone intermediate P, which subsequently reacts with a second equivalent of ketone to yield diolcontaining products 10, 10-d₁₂, and 11. In contrast to the reaction of 6 with CO, none of the Ta starting material is sacrificed in this mechanism, leading to the observed higher yield of 10. Unfortunately, reaction of 6 with H₂ and acetone generates myriad hydride-containing side products, as evidenced by many peaks near 17 ppm in the ¹H NMR spectrum; the presence of these side products prevented monitoring of this reaction by ¹H NMR spectroscopy.

Scheme 8. Proposed mechanism for the formation of diol complexes 10, 10- d_{12} , and 11 from 6, H_2 , and excess ketone.

$$X_3$$
Ta X_3

To provide insight into the reactivity observed with H_2 , we carried out a crossover experiment with acetone- d_6 . Reaction of 6 with H_2 and 1:1 acetone:acetone- d_6 in benzene led to isolation of a ca. 1:2:1 mixture of isotopologues 10, 10- d_6 , and 10- d_{12} (Scheme 9, Figures S69-73, p. S31). Whereas the reaction between 6 and CO *always* generates proteo- η^2 -acetone intermediate **J** (Scheme 6), formation of η^2 -acetone intermediate **P** via reaction of 6 with H_2 and equimolar acetone:acetone- d_6 is equally likely to occur with proteo- or deutero-acetone (assuming a negligible secondary kinetic isotope effect). The reaction of a 1:1 mixture of proteo:deutero η^2 -acetone intermediate **P** with a second equivalent of acetone or acetone- d_6 leads to the observed statistical distribution of products.

Scheme 9. Synthesis of a ca. 1:2:1 mixture of complexes 10, 10- d_6 , and 10- d_{12} from the reaction of 6 with H_2 and 1:1 acetone:acetone- d_6 .

Conclusion

Overall, we have demonstrated that successive transfer of methyl groups from di-, tri-, and tetramethyl Ta(V) precursors to unsaturated small molecule substrates is a viable strategy to access a plethora of organic and organometallic products bearing new C-C bonds. Addition of CO or CNXyl to Ta(V) tri- and tetramethyl complexes 1-X (X = Me, Cl) led to the formation of Ta(V) oxo or imido products containing enolate (2-X) or enamine (3) ligands. Enolate complexes 2-X could add trimethylsilyl chloride across Ta-oxo groups to yield complexes 4-X, providing rare examples of 1,2-addition across early transition metal-oxo multiple bonds. We were able to protonate the enamine ligand of 3 to give the corresponding free imine 5. In contrast to these results, reaction of 1-Cl with CNXyl resulted in noninnocent ligand behavior, yielding a variety

of organometallic products bearing a chiral, dianionic scorpionate ligand, as well as organic side products. Migratory insertion of one equivalent of CNXyl into a Ta-Me bond, followed by insertion of the newly formed XylNCMe group into a B-H bond of the bis(NHC)borate ligand, produced dimethyl chloro scorpionate complex 6. Additional equivalents of CNXyl led to the azaallyl hydrido scorpionate complex 7 and the imido isocyanide scorpionate complex 8, as well as the generation of organic side products propene and xylyl ketenimine 9. Finally, we were able to observe a unique pathway to pinacol-containing products: addition of CO to 6 resulted in formation of acetone via sequential methyl transfers from the Ta metal center to CO. Two equivalents of CO-generated acetone could be reductively coupled across the Ta center to form pinacol product 10. Diol-containing products 10, $10-d_{12}$, and the ethyl derivative 11 were also accessed via the reaction of 6 with H₂ and excess ketone. Using a variety of NMR-monitored experiments and labeling studies, we propose plausible mechanisms for these coupling reactions. Our work builds upon several prior reports in this arena, but stands alone in that both acetone formation and reductive pinacol coupling were observed over the course of a single reaction. Future work will focus on accessing and harnessing the reducing ability of transient Ta(III) intermediate **O**, which can be generated from the reaction of **6** with H₂.

Experimental

General Considerations. Unless otherwise stated, all reactions were performed under an atmosphere of dry N₂ using standard Schlenk line techniques or in an MBraun inert atmosphere glovebox under an atmosphere of nitrogen (<1.0 ppm O₂/H₂O). All glassware, cannulae, and Celite were stored in an oven at ca. 150 °C for at least 12 h prior to use. Molecular sieves (3 Å) were activated by heating to 200 °C overnight under vacuum and then stored in a glovebox. NMR

spectra were obtained at ambient temperature, unless otherwise noted, using Bruker AV-300, AVB-400, AV-500, and AV-600 spectrometers. ¹H and ¹³C{¹H} NMR chemical shifts (δ) were reported relative to residual solvent peaks. ¹¹B NMR chemical shifts (δ) were referenced to an external standard (BF₃·Et₂O). ²H NMR chemical shifts (δ) were referenced to an internal standard (toluene-d₈). ¹H and ¹³C NMR assignments were routinely confirmed by ¹H-¹³C HSQC NMR experiments. Fourier transform infrared (FT-IR) samples were prepared as Nujol mulls and were taken between KBr disks using a Nicolet iS10 FT-IR spectrometer. Melting points were determined using an Optimelt SRS automated melting point system using sealed capillaries prepared under an atmosphere of dry N₂. Elemental analysis samples were sealed under vacuum in ampules and analyzed at the University of California, Berkeley. Mass spectrometry analyses were carried out at the QB3 Mass Spectrometry Faculty at the University of California, Berkeley; samples were analyzed by an AutoSpec Premier mass spectrometer (Waters, Manchester, UK), equipped with an electron impact ion source and Masslynx software. The sample was introduced by a direct probe without heating and the low resolution data was acquired at a mass range from 50 to 1100 m/z.

Materials. Diethyl ether (Et₂O), *n*-hexane, toluene, benzene, and tetrahydrofuran (THF) were dried and degassed using a Phoenix solvent drying system commercially available from JC Meyer Solvent Systems. Hexamethyldisiloxane (HMDSO) was dried using sodium/benzophenone, degassed with three freeze-pump-thaw cycles, and vacuum-transferred prior to storage in a glovebox over molecular sieves. Toluene-*d*₈ and C₆D₆ were obtained from Cambridge Isotope Laboratories and dried using sodium/benzophenone, degassed with three freeze-pump-thaw cycles, and vacuum-transferred or distilled prior to storage in a glovebox over molecular sieves. [H₂B(^{Mes}Im)₂]TaMe₄ (1-Me),²⁸ [H₂B(^{Mes}Im)₂]TaMe₃Cl (1-Cl),²⁸ and 2,6-diisopropylphenyl

isocyanide⁸² were prepared according to literature procedures. All other reagents were acquired from commercial sources and used as received.

Warning! Carbon monoxide (CO) is a highly toxic, odorless, colorless, flammable gas. Manipulations using CO gas should be carried out entirely within a calibrated fume hood (or an equivalently contained, mechanically ventilated area) by qualified personnel only.

Synthetic Procedures.

 $[H_2B(^{Mes}Im)_2]TaO(Me)[OC(Me)=C(Me)_2]$ (2-Me). Compound 1-Me·toluene (259 mg, 0.360 mmol) was added to a 250 mL round-bottomed Schlenk flask and dissolved in benzene (15 mL). The solution was degassed, and the headspace was refilled with CO. After 15 minutes, the solution changed color from pale yellow to orange. The flask was sealed, and the solution was stirred vigorously at ambient temperature for 2.5 h. Then, the volatiles were removed via lyophilization, resulting in an orange-colored powder. The crude product was extracted with toluene (2 x 6 mL), and the resulting solution was filtered through Celite, concentrated to a final volume of ca. 2 mL, and stored at -40 °C overnight, yielding pale yellow crystals of 2-Me (186 mg, 76% yield). X-ray quality crystals of 2-Me were grown from a saturated toluene solution of 2-Me at -40 °C. ¹H NMR (600 MHz, 298 K, C₆D₆): δ 7.09 (s, HC_{Imid}, 2H), 6.81 (br s, HC_{Mes}, 1H), 6.72 (br s, HC_{Mes}, 1H, overlapping HC_{Imid} peak), 6.72 (s, HC_{Imid}, 2H, overlapping HC_{Mes} peak), 6.19 (br s, HC_{Mes}, 1H), 6.11 (br s, HC_{Mes} , 1H), 4.25 (br s, HB, 2H), 2.28 (br s, H_3C_{Mes} , 3H), 2.04 (s, H_3C_{Mes} , 9H), 1.99 (br s, H_3C_{Mes} , 3H), 1.85 (br s, H_3C_{Mes} , 3H), 1.67 (s, OC(Me)=C(Me)₂, 3H), 1.66 (s, OC(Me)=C(Me)₂, 3H), 1.48 (s, OC(Me)=C(Me)₂, 3H), 0.70 (s, TaMe, 3H). ¹³C NMR (151 MHz, 298 K, C₆D₆): δ 149.6, 129.3 (H C_{Imid}), 121.6 (H C_{Mes}), 110.1, 36.3 (TaMe), 21.0 (H₃ C_{Mes}), 18.7 (OC(Me)=C(Me)₂), 18.6 (H₃ C_{Mes}), 17.8 (OC(Me)=C(Me)₂), 17.5 (OC(Me)=C(Me)₂). ¹¹B NMR (193 MHz, 298 K, C_6D_6): $\delta -7.78$ (s). Anal. Calcd for $C_{30}H_{40}BN_4O_2Ta$ (2-Me): C, 52.96; H, 5.93; N, 8.23. Found: C,

53.23; H, 6.07; N, 8.40. FT-IR (KBr, Nujol, cm⁻¹): v_{B-H} 2424 (m), 2370 (w), 2318 (m), 2257 (w), 2235 (w). Mp: 202 °C (dec).

 $[H_2B(^{Mes}Im)_2]TaO(Cl)[OC(Me)=C(Me)_2]$ (2-Cl). Compound 1-Cl·toluene (150 mg, 0.204) mmol) was added to a 250 mL round-bottomed Schlenk flask and dissolved in benzene (10 mL). The solution was degassed, and the headspace was refilled with CO. After 15 minutes, the solution changed color from light brown to yellow. The flask was sealed, and the solution was stirred vigorously at ambient temperature for 2.5 h. Then, the volatiles were removed via lyophilization, resulting in a yellow-colored powder. The crude product was extracted with toluene (2 x 7 mL), and the resulting solution was filtered through Celite, concentrated to a final volume of ca. 8 mL, and stored at -40 °C overnight, yielding bright yellow crystals of 2-Cl (91.4 mg, 64% yield). Xray quality crystals of 2-Cl were grown by vapor diffusion of hexane into a saturated benzene solution of **2-Cl** at room temperature. ¹H NMR (500 MHz, 298 K, C_6D_6): δ 7.01 (d, J = 1.1 Hz, HC_{Imid} , 1H), 6.99 (d, J = 1.1 Hz, HC_{Imid} , 1H), 6.79 (s, HC_{Mes} , 1H), 6.75 (s, HC_{Mes} , 1H), 6.69 (s, HC_{Mes} , 2H), 6.14 (d, J = 0.9 Hz, HC_{Imid} , 1H), 6.02 (d, J = 0.9 Hz, HC_{Imid} , 1H), 4.21 (br s, HB, 2H), 2.23 (s, H_3C_{Mes} , 3H), 2.15 (s, H_3C_{Mes} , 3H), 2.11 (s, H_3C_{Mes} , 3H), 2.04 (s, H_3C_{Mes} , 3H), 2.00 (s, H_3C_{Mes} , 3H), 1.76 (s, H_3C_{Mes} , 3H), 1.66 (s, $OC(Me)=C(Me)_2$, 3H), 1.65 (s, $OC(Me)=C(Me)_2$, 3H), 1.44 (s, OC(Me)=C(Me)₂, 3H). ¹³C NMR (151 MHz, 298 K, C₆D₆): δ 200.6 (C_{Imid}), 194.9 (C_{Imid}), 150.5, 139.0, 138.8, 136.3, 135.9, 135.8, 135.5, 135.3, 129.6, (HC_{Mes}), 129.4, (HC_{Mes}), 129.0 (HC_{Mes}) , 129.0 (HC_{Mes}) , 128.6, 126.9 (HC_{Imid}) , 125.1 (HC_{Imid}) , 122.0 (HC_{Imid}) , 121.7 (HC_{Imid}) , 112.1, 21.0 (H_3C_{Mes}), 21.0 (H_3C_{Mes}), 19.1 (H_3C_{Mes}), 19.0 (H_3C_{Mes}), 18.6 (H_3C_{Mes}), 17.9 $(OC(Me)=C(Me)_2)$, 17.5 $(OC(Me)=C(Me)_2)$, 17.3 $(OC(Me)=C(Me)_2)$. ¹¹B NMR (193 MHz, 298) K, C₆D₆): δ –8.11 (s). Anal. Calcd for C₂₉H₃₇BClN₄O₂Ta (**2-Cl**): C, 49.70; H, 5.32; N, 7.99. Found: C, 50.05; H, 5.63; N, 7.82. FT-IR (KBr, Nujol, cm⁻¹): ν_{B-H} 2436 (m), 2371 (w), 2319 (m), 2262 (w), 2236 (w). Mp: 210 °C (dec).

[H₂B(MesIm)₂]Ta(NXyl)(Me)[NXyl(Me)C=C(Me)₂] (3). Compound 1-Me·toluene (150 mg, 0.209 mmol) was combined with xylyl isocyanide (2 eq., 54.8 mg, 0.418 mmol) in a 20 mL glass scintillation vial in the glovebox. The solid mixture was dissolved in toluene (8 mL), resulting in an immediate color change from pale yellow to dark orange. The vial was sealed, and the solution was stirred vigorously at ambient temperature for 1 h. The volatile materials were removed under vacuum, and the oily orange solids were triturated with hexane (2 x 4 mL), affording orange, amorphous solids. The solids were extracted with THF (2 x 4 mL), and the resulting solution was filtered through Celite, concentrated to a final volume of ca. 0.5 mL, and stored at -40 °C overnight, yielding dark orange crystals of 3 (168 mg, 91% yield). X-ray quality crystals of 3 were grown from a saturated Et₂O solution of **3** at -40 °C. ¹H NMR (600 MHz, 298 K, C₆D₆): δ 7.29 (s, HC_{Ar} , 1H), 7.12 (s, HC_{Ar} , 1H), 6.95 (d, J = 6.7 Hz, $m-HC_{Xvl}$, 1H), 6.73 (s, HC_{Ar} , 1H), 6.71 (d, $J = 6.8 \text{ Hz}, m\text{-}HC_{Xvl}, 1H), 6.69 \text{ (s, }HC_{Ar}, 1H), 6.64 \text{ (t, }J = 6.9 \text{ Hz, }o\text{-}HC_{Xvl}, 1H), 6.59 \text{ (d, }J = 6.8 \text{ Hz, }g)$ Hz, m- HC_{XVI} , 1H), 6.49 (t, J = 7.6 Hz, o- HC_{XVI} , 1H), 6.40 (d, J = 6.8 Hz, m- HC_{XVI} , 1H), 6.34 (s, HC_{Ar}, 1H), 6.21 (s, HC_{Ar}, 1H), 6.17 (s, HC_{Ar}, 1H), 6.10 (s, HC_{Ar}, 1H), 4.61 (br s, HB, 1H), 4.19 (br s, HB, 1H), 2.28 (s, H_3C_{Ar} , 3H), 2.18 (s, H_3C_{Ar} , 3H), 2.13 (s, H_3C_{Ar} , 6H), 2.08 (s, H_3C_{Ar} , 3H), 1.97 (s, H_3C_{Ar} , 3H), 1.85 (s, H_3C_{Ar} , 3H), 1.76 (s, NXyl(Me)C=C(Me)₂, 3H), 1.73 (s, $NXyI(Me)C=C(Me)_2$, 3H), 1.69 (s, H_3C_{Ar} , 3H), 1.63 (s, H_3C_{Ar} , 3H), 1.56 (s, H_3C_{Ar} , 3H), 1.08 (s, TaMe, 3H), 1.07 (s, NXyl(Me)C=C(Me)₂, 3H). 13 C NMR (151 MHz, 298 K, C₆D₆): δ 207.2 (C_{Imid}), $202.1 (C_{\text{Imid}}), 155.5, 152.1, 140.0, 138.9, 138.4, 137.6, 137.3, 137.2, 137.0, 136.3, 134.8, 133.9,$ 133.7, 132.0, 131.3, 129.5 (H C_{Ar}), 129.1 (H C_{Ar}), 128.8 (m-H C_{Xyl}), 128.6 (m-H C_{Xyl}), 128.4 (H C_{Ar}), 128.0 (H C_{Ar}), 126.4 (m-H C_{Xyl}), 125.5 (m-H C_{Xyl}), 124.4 (H C_{Ar}), 122.9 (H C_{Ar}), 122.6 (o-H C_{Xyl}),

121.9 (o-HC_{Xyl}), 121.4 (HC_{Ar}), 108.0, 47.7 (TaMe), 22.3 (H₃C_{Ar}), 21.5 (H₃C_{Ar}), 21.2 (H₃C_{Ar}), 21.0 (H_3C_{Ar}) , 20.8 (H_3C_{Ar}) , 20.5 (H_3C_{Ar}) , 20.0 (H_3C_{Ar}) , 19.5 $(NXyl(Me)C=C(Me)_2)$, 19.3 (H_3C_{Ar}) , 19.1 $(NXyl(Me)C=C(Me)_2)$, 18.7 $(NXyl(Me)C=C(Me)_2)$, 17.1 (H_3C_{Ar}) . ¹¹B NMR (193 MHz, 298 K, C_6D_6): $\delta -7.61$ (s). Anal. Calcd for $C_{46}H_{58}BN_6Ta$ (3): C, 62.31; H, 6.59; N, 9.48. Found: C, 62.42; H, 6.30; N, 9.42. FT-IR (KBr, Nujol, cm⁻¹): v_{B-H} 2411 (m), 2363 (w), 2272 (w). Mp: 194 °C (dec). [H₂B(MesIm)₂]TaMeCl(OSiMe₃)[OC(Me)=C(Me)₂] (4-Me). In a 20 mL glass scintillation vial in an inert atmosphere glovebox, compound 2-Me (100 mg, 0.147 mmol) was dissolved in toluene (8 mL), resulting in a pale-yellow solution. The solution was set to stir at room temperature; then, excess chlorotrimethylsilane (4 eq., 74.6 µL, 0.588 mmol) was added via micropipette, resulting in an immediate color change from pale yellow to yellow. The vial was sealed, and the solution was stirred vigorously at ambient temperature for 30 minutes. The volatile materials were removed under vacuum, and the oily yellow solids were triturated with hexane (2 x 2 mL), affording yellow, powdery solids. The solids were extracted with Et₂O (2 x 3 mL), and the resulting solution was filtered through Celite, concentrated to a final volume of ca. 0.5 mL, and stored at -40 °C overnight, yielding yellow crystals of 4-Me (98.4 mg, 85% yield). X-ray quality crystals of 4-Me were grown from a saturated Et₂O solution of 4-Me at -40 °C. Compound 4-Me exists as a 1:1 mixture of fac and mer isomers at -70 °C; these isomers rapidly interconvert on the NMR timescale at 40 °C. ¹H NMR (600 MHz, 298 K, C₆D₆): δ 7.26 (br s, HC_{Imid}, 2H), 6.71 (br s, HC_{Mes}, 4H), 6.11 (br s, HC_{Imid} , 2H), 4.38 (br s, HB, 2H), 2.07 (br s, H_3C_{Mes} , 18H), 1.78 (s, $OC(Me) = C(Me)_2$, 3H), 1.50 (br s, OC(Me)= $C(Me)_2$, 6H), 1.03 (br s, TaMe, 3H), 0.20 (br s, SiMe, 9H). ¹H NMR (500) MHz, 313 K, tol-d₈): δ 7.22 (s, HC_{Imid}, 2H), 6.69 (s, HC_{Mes}, 4H), 6.16 (s, HC_{Imid}, 2H), 4.24 (br s, HB, 2H), 2.04 (s, H_3C_{Mes} , 18H, overlapping tol- d_8 methyl resonance), 1.74 (s, OC(Me)=C(Me)₂, 3H), 1.53 (s, OC(Me)= $C(Me)_2$, 3H), 1.51 (br s, OC(Me)= $C(Me)_2$, 3H), 0.97 (br s, TaMe, 3H), 0.16

(s, SiMe, 9H). ¹H NMR (500 MHz, 203 K, tol-d₈): δ 7.32 (s, HC_{Imid}, 1H), 7.17 (s, HC_{Imid}, 1H), 7.15 ((, HC_{Imid} , 1H, overlapping tol- d_8 aryl resonance), 7.12 (s, HC_{Imid} , 1H), 6.71 (s, HC_{Mes} , 3H), 6.63 (s, HC_{Mes}, 1H), 6.61 (s, HC_{Mes}, 1H), 6.54 (s, HC_{Mes}, 1H), 6.51 (s, HC_{Mes}, 1H), 6.34 (s, HC_{Mes}, 1H), 5.87 (s, HC_{Imid}, 1H), 5.66 (s, HC_{Imid}, 1H), 5.64 (s, HC_{Imid}, 1H), 5.63 (s, HC_{Imid}, 1H), 4.57 (br d, J = 63 Hz, HB, 2H), 4.40 (br d, J = 52 Hz, HB, 2H), 2.33 (s, H_3C_{Mes} , 3H), 2.21 (s, H_3C_{Mes} , 6H), 2.20 (s, H_3C_{Mes} , 3H), 2.14 (s, H_3C_{Mes} , 3H), 2.12 (s, H_3C_{Mes} , 3H), 2.08 (s, H_3C_{Mes} , 3H, overlapping tol- d_8 methyl resonance), 2.05 (s, H_3C_{Mes} , 3H), 2.01 (s, H_3C_{Mes} , 3H), 1.95 (s, H_3C_{Mes} , 3H), 1.89 (s, H_3C_{Mes} , 3H), 1.83 (s, H_3C_{Mes} , 3H), 1.81 (s, OC(Me)=C(Me)₂, 3H), 1.77 (s, OC(Me)=C(Me)₂, 3H), 1.76 (s, $OC(Me)=C(Me)_2$, 3H), 1.68 (s, $OC(Me)=C(Me)_2$, 3H), 1.62 (s, TaMe, 3H), 1.34 (s, $OC(Me)=C(Me)_2$, 3H), 1.29 (s, $OC(Me)=C(Me)_2$, 3H), 0.92 (s, TaMe, 3H), 0.38 (s, SiMe, 9H), -0.04 (s, SiMe, 9H). ¹³C NMR (151 MHz, 298 K, C₆D₆): δ 138.2, 129.1 (HC_{Mes}), 128.4 (HC_{Mes}), $128.1 \text{ (H}C_{\text{Mes}}), 128.0 \text{ (H}C_{\text{Mes}}), 126.2 \text{ (H}C_{\text{Imid}}), 121.8 \text{ (H}C_{\text{Imid}}), 21.0 \text{ (H}_3C_{\text{Mes}}), 19.1 \text{ (H}_3C_{\text{Mes}}), 18.5$ $(OC(Me)=C(Me)_2)$, 18.4 $(OC(Me)=C(Me)_2)$, 1.9 (SiMe). ¹³C NMR (126 MHz, 313 K, tol- d_8): δ 138.1, 129.2 (H C_{Mes}), 128.3 (H C_{Mes}), 126.1 (H C_{Imid}), 121.7 (H C_{Imid}), 21.0 (H₃ C_{Mes}), 19.0 (H₃ C_{Mes}), 18.5 (OC(Me)=C(Me)₂), 18.4 (OC(Me)=C(Me)₂), 1.9 (SiMe). ¹³C NMR (126 MHz, 203 K, tol- d_8): δ 193.0 (C_{Imid}), 190.8 (C_{Imid}), 189.2 (C_{Imid}), 188.3 (C_{Imid}), 151.6, 149.4, 138.7, 137.8, 136.4 (HC_{Mes}), 136.2 (HC_{Mes}), 136.1 (HC_{Mes}), 136.0 (HC_{Mes}), 135.9 (HC_{Mes}), 135.4 (HC_{Mes}), 135.1 (HC_{Mes}), 135.0 (HC_{Mes}), 126.1 (HC_{Imid}), 126.0 (HC_{Imid}), 125.9 (HC_{Imid}), 125.7 (HC_{Imid}), 121.9 (HC_{Imid}), 121.7 (HC_{Imid}) , 121.5 (HC_{Imid}) , 120.7 (HC_{Imid}) , 114.4, 111.7, 59.6, 42.3, 19.5 (H_3C_{Mes}) , 19.2 (H_3C_{Mes}) , 19.1 (H_3C_{Mes}), 18.9 (H_3C_{Mes}), 18.7 (H_3C_{Mes}), 18.6 (H_3C_{Mes}), 18.2 ($OC(Me)=C(Me)_2$), 18.0 $(OC(Me)=C(Me)_2)$, 17.8 $(OC(Me)=C(Me)_2)$, 17.7 $(OC(Me)=C(Me)_2)$, 14.9, 1.8 (SiMe), 1.7 (SiMe). ¹¹B NMR (193 MHz, 298 K, C₆D₆): δ –5.36 (s). ¹¹B NMR (160 MHz, 313 K, tol- d_8): δ -5.93 (s). ¹¹B NMR (160 MHz, 203 K, tol- d_8): δ -2.82 (s), -7.55 (s). Anal. Calcd for C₃₃H₄₉BClN₄O₂SiTa (**4-Me**): C, 50.23; H, 6.26; N, 7.10. Found: C, 50.19; H, 6.40; N, 6.93. FT-IR (KBr, Nujol, cm⁻¹): v_{B-H} 2404 (m), 2320 (w), 2267 (w). Mp: 166 °C (dec).

[H₂B(MesIm)₂]TaCl₂(OSiMe₃)[OC(Me)=C(Me)₂] (4-Cl). In a 20 mL glass scintillation vial in an inert atmosphere glovebox, compound 2-Cl (100 mg, 0.143 mmol) was dissolved in toluene (8 mL), resulting in a bright yellow solution. The solution was set to stir at room temperature; then, excess chlorotrimethylsilane (4 eq., 72.4 µL, 0.571 mmol) was added via micropipette, resulting in an immediate color change from bright yellow to yellow-orange. The vial was sealed, and the solution was stirred vigorously at ambient temperature for 30 minutes. The volatile materials were removed under vacuum, and the oily yellow solids were triturated with hexane (2 x 2 mL), affording yellow, powdery solids. The solids were extracted with Et₂O (2 x 5 mL), and the resulting solution was filtered through Celite, concentrated to a final volume of ca. 1 mL, and stored at -40 °C overnight, yielding yellow crystals of 4-Cl (83.8 mg, 73% yield). X-ray quality crystals of 4-CI were grown from a saturated Et₂O solution of 4-CI at -40 °C. ¹H NMR (600 MHz, 298 K, C₆D₆): δ 7.24 (s, HC_{Imid}, 1H), 7.11 (s, HC_{Imid}, 1H), 6.74 (s, HC_{Mes}, 2H), 6.64 (s, HC_{Mes}, 1H), 6.47 (s, HC_{Mes}, 1H), 6.21 (s, HC_{Imid}, 1H), 5.95 (s, HC_{Imid}, 1H), 4.44 (br s, HB, 2H), 2.29 (s, H₃C_{Mes}, 3H), 2.19 (s, H_3C_{Mes} , 3H), 2.12 (s, H_3C_{Mes} , 3H), 2.02 (s, $OC(Me) = C(Me)_2$, 3H), 2.00 (s, H_3C_{Mes} , 3H), 1.83 (s, H_3C_{Mes} , 3H), 1.81 (s, H_3C_{Mes} , 3H), 1.37 (s, $OC(Me)=C(Me)_2$, 3H), 1.30 (s, OC(Me)=C(Me)₂, 3H), 0.38 (s, SiMe, 9H). 13 C NMR (151 MHz, 298 K, C₆D₆): δ 193.4 (C_{Imid}), 191.8 (C_{Imid}), 153.1, 138.4, 138.2, 137.7, 136.9, 136.5, 136.4, 136.13, 136.06, 129.4 (HC_{Imid}), 129.3 (HC_{Imid}), 128.6 (HC_{Imid}), 128.5, 128.4 (HC_{Imid}), 128.1, 128.0, 126.1 (HC_{Mes}), 125.9 (HC_{Mes}), 121.9 (H C_{Mes}), 121.0 (H C_{Mes}), 117.9, 21.0 (OC(Me)=C(Me)₂), 20.9 (H₃ C_{Mes}), 19.54 (H₃ C_{Mes}), 19.45 (H_3C_{Mes}), 19.1 (H_3C_{Mes}), 18.5 (H_3C_{Mes}), 18.3 (H_3C_{Mes}), 18.0 ($OC(Me)=C(Me)_2$), 15.1 $(OC(Me)=C(Me)_2)$, 1.9 (SiMe). ¹¹B NMR (193 MHz, 298 K, C₆D₆): δ –5.45 (s). Anal. Calcd for C₃₂H₄₆BCl₂N₄O₂SiTa (**4-Cl**): C, 47.48; H, 5.73; N, 6.92. Found: C, 47.76; H, 5.95; N, 6.75. FT-IR (KBr, Nujol, cm⁻¹): v_{B-H} 2405 (m), 2772 (w). Mp: 182 °C (dec).

N-(1,2-Dimethylpropylidene)-2,6-dimethylbenzenamine (5). In an inert atmosphere glovexbox, compound 3 (15.0 mg, 0.0169 mmol) was combined with lutidinium chloride (2 eq., 4.9 mg, 0.0338 mmol) in a 4 mL glass dram vial. C₆D₆ (0.25 mL) was added to the solid mixture and the resulting orange solution with suspended solids was transferred to a J. Young NMR tube. The tube was sealed and sonicated for 1 day, resulting in a heterogeneous, pale orange solution with tan precipitate. The solution was filtered through Celite and transferred to a clean J. Young NMR tube for NMR analysis, revealing imine 5 and lutidine. Then, the volatiles were removed under vacuum and the solid mixture was analyzed by LRMS. A 20:1 ratio of E:Z-isomers was observed in the ¹H NMR spectrum; in the ¹H NMR spectrum, the aromatic resonances for the Zisomer could not be confidently assigned. ¹H NMR (600 MHz, 298 K, C₆D₆): E-isomer δ 7.05 (m, $m-HC_{Xvl}$, 2H, overlapping lutidine $o-HC_{Ar}$), 6.93 (dd, J = 7.0 Hz, 8.1 Hz, $o-HC_{Xyl}$, 1H), 2.39 (sept, J = 6.8 Hz, N=C(Me)-CH(Me)₂, 1H, overlapping lutidine H_3C_{Ar}), 1.98 (s, H_3C_{Xyl} , 6H), 1.27 (s, 3H. $N=C(Me)-CH(Me)_2$, overlapping Z-isomer $N=C(Me)-CH(Me)_2$, 1.12 (s, N=C(Me)-CH(Me)₂, 3H), 1.11 (s, N=C(Me)-CH(Me)₂, 3H). Z-isomer δ 2.28 (sept, J = 6.8 Hz, $N=C(Me)-CH(Me)_2$, 1H), 2.06 (s, H_3C_{Xyl} , 6H), 1.26 (s, $N=C(Me)-CH(Me)_2$, 3H, overlapping Eisomer $N=C(Me)-CH(Me)_2$, 0.64 (s, $N=C(Me)-CH(Me)_2$, 3H), 0.63 (s, $N=C(Me)-CH(Me)_2$, 3H). ¹³C NMR (151 MHz, 298 K, C_6D_6): *E*-isomer δ 174.3 (N=C(Me)-CH(Me)₂), 149.7 (N- C_{Xvl}), 128.3 (m-H C_{Xyl} , overlapping C₆D₆), 125.6 (p- C_{Xyl}), 122.7 (o-H C_{Xyl}), 38.9 (N=C(Me)-CH(Me)₂), $20.2 \text{ (N=C(Me)-CH(Me)_2)}, 18.0 \text{ (H}_3C_{Xvl}), 17.6 \text{ (N=C(Me)-CH(Me)_2)}.$ Resonances corresponding to the Z-isomer could not be observed by ¹³C NMR. LRMS (EI) m/z: [M]⁺ calcd for C₁₃H₁₉N (**5**): 189.15; Found: 189.

[H(CH(Me)NXvl)B(MesIm)2]TaClMe2 (6). Compound 1-Cl·toluene (1.04 g, 1.42 mmol) was added to a 250 mL round-bottomed Schlenk flask and dissolved in Et₂O (100 mL). Xylyl isocyanide (186 mg, 1.42 mmol) was added to a 50 mL round-bottomed Schlenk flask and dissolved in Et₂O (15 mL). Both solutions were set to stir and cooled to -40 °C; then, the colorless xylyl isocyanide solution was added dropwise via syringe over a period of 10 minutes to the yellow solution of 1-Cl·toluene, resulting in a color change from yellow to dark yellow. The flask was sealed, and the reaction mixture was warmed to -10 °C and then stirred vigorously for 1.5 h. Then, the volatile materials were removed under vacuum, yielding powdery yellow-orange solids. The solids were extracted with Et₂O (3 x 30 mL), and the resulting yellow-orange solution was filtered through Celite and concentrated to a final volume of ca. 15 mL. Yellow microcrystals began to form on the sides of the flask; the solution was allowed to sit undisturbed at room temperature for 30 minutes before storing at -40 °C overnight, yielding yellow microcrystals of 6 (740 mg, 67%) yield). X-ray quality crystals of 6 were grown from a saturated Et₂O solution of 6 at -40 °C. ¹H NMR (600 MHz, 298 K, C₆D₆): δ 7.24 (d, J = 1.3 Hz, HC_{Im} , 1H), 7.13 (d, J = 1.3 Hz, HC_{Im} , 1H), 7.11 (br d, J = 7.0 Hz, $m-HC_{Xvl}$, 1H), 7.04 (br d, J = 6.9 Hz, $m-HC_{Xvl}$, 1H), 7.00 (t, J = 7.5 Hz, o- HC_{Xvl} , 1H), 6.77 (br s, HC_{Mes} , 1H), 6.71 (s, HC_{Mes} , 1H), 6.65 (s, HC_{Mes} , 1H), 6.62 (br s, HC_{Mes} , 1H), 6.20 (s, HC_{Im} , 1H), 6.14 (s, HC_{Im} , 1H), 4.25 (br s, HB, 1H), 3.93 (q, J = 7.0 Hz, $H(CH(Me)NXyl)B(^{Mes}Im)_2$, 1H), 2.49 (s, H_3C_{Ar} , 3H), 2.11 (br s, H_3C_{Ar} , 3H), 2.06 (br s, H_3C_{Ar} , 3H), 2.02 (s, H₃C_{Ar}, 3H), 2.00 (s, H₃C_{Ar}, 3H), 1.94 (s, H₃C_{Ar}, 3H), 1.80 (s, H₃C_{Ar}, 3H), 1.08 (d, J = 7.2 Hz, $H(CH(Me)NXy1)B(^{Mes}Im)_2$, 3H), 1.04 (br s, TaMe, 3H), 0.82 (br s, TaMe, 3H). ¹³C NMR $(151 \text{ MHz}, 298 \text{ K}, C_6D_6)$: δ 140.9, 139.7, 138.4, 138.3, 137.1, 137.0, 136.6, 136.2, 136.0, 135.7, 130.2 (m-H C_{Xyl}), 129.1 (H C_{Mes}), 128.9 (H C_{Mes}), 128.8 (m-H C_{Xyl}), 128.7 (H C_{Mes}), 128.4 (H C_{Mes}), 127.6 (o-H C_{Xvl}), 124.6 (H C_{Imid}), 124.3 (H C_{Imid}), 122.1 (H C_{Imid}), 121.8 (H C_{Imid}), 57.7

(H(*C*H(Me)NXyl)B(^{Mes}Im)₂), 22.2 (H₃*C*_{Ar}), 21.0 (H₃*C*_{Ar}), 20.9 (H₃*C*_{Ar}), 20.3 (H₃*C*_{Ar}), 19.2 (H₃*C*_{Ar}), 18.9 (H₃*C*_{Ar}), 18.8 (H₃*C*_{Ar}), 18.1 (H(CH(*Me*)NXyl)B(^{Mes}Im)₂). ¹¹B NMR (193 MHz, 298 K, C₆D₆): δ 0.35 (s). Anal. Calcd for C₃₆H₄₆BClN₅Ta (**6**): C, 55.72; H, 5.98; N, 9.03. Found: C, 55.81; H, 5.97; N, 8.82. FT-IR (KBr, Nujol, cm⁻¹): ν_{B-H} 2404 (w), 2378 (m). Mp: 98 °C (dec).

[H(CH(Me)NXyl)B(MesIm)2]TaClH[NXylC(Me)CH2] (7). In a 20 mL glass scintillation vial, compound 1-Cl·toluene (156 mg, 0.212 mmol) was dissolved in toluene (4 mL); in a separate vial, xylyl isocyanide (55.7 mg, 0.425 mmol) was dissolved in toluene (4 mL). Both vials were cooled to -78 °C with stirring in a cold well in an inert atmosphere glovebox. Then, the colorless xylyl isocyanide solution was added dropwise to the yellow solution of 1-Cl·toluene over a period of 5 min; over the course of the addition, the yellow solution darkened to orange. After the addition, the vial was sealed and stirred vigorously at -78 °C for 2 h. The vial was removed from the cold well and allowed to warm to ambient temperature; upon warming, the color of the solution darkened to red. The volatile materials were removed under vacuum, and the oily red solids were triturated with hexane (2 x 3 mL), affording red, amorphous solids. The solids were extracted with Et₂O (2 x 5 mL), and the resulting solution was filtered through Celite, concentrated to a final volume of ca. 0.5 mL, and stored at -40 °C overnight, yielding dark orange crystals of 7 (106 mg, 55% yield). X-ray quality crystals of 7 were grown from a saturated Et₂O solution of 7 at -40 °C. ¹H NMR (600 MHz, 298 K, C₆D₆): δ 17.34 (d, ³J = 3.3 Hz, TaH, 1H), 7.43 (s, HC_{Imid} , 1H), 7.22 (s, HC_{Imid} , 1H), 7.10 (d, J = 7.4 Hz, $m-HC_{XvI}$, 1H), 6.95 (s, HC_{Mes} , 1H), 6.91 (t, J = 7.6 Hz, o- HC_{Xvl} , 1H, overlapping HC_{Mes}), 6.89 (s, HC_{Mes} , 1H, overlapping o- HC_{Xvl}), 6.83-6.75 (m, HC_{Mes} and HC_{Xvl} , 6H), 6.31 (s, HC_{Imid} , 1H), 6.27 (s, HC_{Imid} , 1H), 4.21 (br s, $H(CH(Me)NXyl)B(^{Mes}Im)_2$, 1H), 3.94 (s, NXylC(Me)C H_2 , 1H), 3.38 (q, J = 6.7 Hz, H(CH(Me)NXyl)B(Mes Im)₂, 1H), 3.02 (d, $^{3}J = 3.3 \text{ Hz}$, NXylC(Me)C H_{2} , 1H), 2.30 (s, $H_{3}C_{Ar}$, 3H), 2.23 (s, $H_{3}C_{Ar}$, 3H), 2.20 (s, $H_{3}C_{Ar}$, 3H),

2.11 (s, H_3C_{Ar} , 6H), 2.09 (s, H_3C_{Ar} , 3H), 2.06 (s, H_3C_{Ar} , 3H), 2.01 (s, H_3C_{Ar} , 3H), 1.93 (s, H_3C_{Ar} , 3H), 1.40 (s, H_3C_{Ar} , 3H), 0.87 (d, J = 6.6 Hz, H(CH(Me)NXyl)B(MesIm)₂, 3H), 0.82 (s, NXylC(Me)CH₂, 3H). 13 C NMR (151 MHz, 298 K, C₆D₆): δ 194.9 (C_{Imid}), 191.4 (C_{Imid}), 156.4, 153.1, 148.4, 139.0, 138.2, 138.1, 137.6, 137.5, 137.3, 136.4, 136.2, 135.9, 135.2, 134.8, 130.1, 129.7 (HC_{Ar}), 129.4 (HC_{Mes}), 129.2 (HC_{Ar}), 129.3 (HC_{Ar}), 129.1 (HC_{Ar}), 128.9 (HC_{Mes}), 128.4 (HC_{Mes}), 127.2 (HC_{Ar}), 125.6 (o-HC_{Xyl}), 125.0 (m-HC_{Xyl}), 124.6 (HC_{Imid}), 124.1 (HC_{Imid}), 122.5 (HC_{Imid}), 121.4 (HC_{Imid}), 70.5 (NXylC(m)CH₂), 68.1 (H(CH(m)NXyl)B(m)(m), 19.2 (H(CH(m)NXyl)B(m), 21.1 (H₃C_{Ar}), 21.0 (H₃C_{Ar}), 19.8 (H₃C_{Ar}), 19.5 (H₃C_{Ar}), 19.2 (H(CH(m)NXyl)B(m), 19.1 (H₃C_{Ar}), 18.8 (H₃C_{Ar}), 18.7 (NXylC(m)CH), 18.5 (H₃C_{Ar}), 18.3 (H₃C_{Ar}). m1 NMR (193 MHz, 298 K, C₆D₆): m0.30 (s). Anal. Calcd for C₄5H₅5BClN₆Ta (7): C, 59.58; H, 6.11; N, 9.26. Found: C, 59.56; H, 5.91; N, 9.17. FT-IR (KBr, Nujol, cm⁻¹): v_{B-H} 2374 (m). Mp: 172 °C (dec).

Generation of 7 in solution from 6. In a 20 mL glass scintillation vial in an inert atmosphere glovebox, compound 6 (15.0 mg, 0.0193 mmol) was dissolved in C₆D₆ (0.25 mL) and the resulting yellow solution was set to stir. In a separate vial, xylyl isocyanide (1 eq., 2.5 mg, 0.0193 mmol) was dissolved in C₆D₆ (0.25 mL) and then the colorless solution was added in one portion to the solution of 6, resulting in an immediate color change to dark orange. The dark orange solution was transferred to a J. Young NMR tube; subsequent ¹H NMR analysis revealed complete and clean conversion to 7. The ¹H NMR spectrum of 7 prepared via this route exactly matched that of isolated 7.

[H(CH(Me)NXyl)B(MesIm)2]TaCl(N-Xyl)(CN-Xyl) (8). In a 20 mL glass scintillation vial in an inert atmosphere glovebox, compound 1-Cl·toluene (150 mg, 0.212 mmol) was dissolved in toluene (4 mL); in a separate vial, xylyl isocyanide (111 mg, 0.850 mmol) was dissolved in toluene

(4 mL). The yellow solution of **1-Cl·toluene** was set to stir at room temperature and the colorless solution of xylyl isocyanide was added in one portion, resulting in an immediate color change to dark red. The vial was sealed, and the solution was stirred vigorously at ambient temperature for 1 h. The volatile materials were removed under vacuum, and the oily red solids were triturated with hexane (2 x 5 mL), affording red, amorphous solids. The solids were extracted with Et₂O (2 x 6 mL), and the resulting solution was filtered through Celite, concentrated to a final volume of ca. 3 mL, and allowed to sit undisturbed at ambient temperature for 4 h before storing at -40 °C overnight, yielding dark orange crystals of 8 (164 mg, 77% yield). X-ray quality crystals of 8 were grown from a saturated Et₂O solution of 8 at -40 °C. Compound 8 exists as a 1:1 mixture of two diastereotopic pairs of enantiomers in solution at room temperature. ¹H NMR (600 MHz, 298 K, toluene-d8): δ 7.29 (d, J = 1.4 Hz, HC_{Ar} , 1H), 7.26 (d, J = 1.4 Hz, HC_{Ar} , 1H), 7.23 (d, J = 1.4 Hz, HC_{Ar} , 1H), 7.15 (d, J = 1.4 Hz, HC_{Ar} , 1H), 7.05 (br t, J = 7.1 Hz, $o-HC_{Xvl}$, 2H), 7.02 (d, J = 1.2Hz, HC_{Ar} , 1H), 6.93 (s, HC_{Ar} , 1H), 6.92 (s, HC_{Ar} , 1H), 6.87 (br t, J = 7.4 Hz, $o-HC_{Xyl}$, 2H), 6.77 (s, HC_{Ar}, 1H), 6.75 (s, HC_{Ar}, 1H), 6.72 (br s, HC_{Ar}, 3H), 6.67 (br s, HC_{Ar}, 2H), 6.64 (s, HC_{Ar}, 1H), 6.63 (s, HC_{Ar}, 2H), 6.59 (s, HC_{Ar}, 1H), 6.58 (s, HC_{Ar}, 1H), 6.57 (br s, HC_{Ar}, 2H), 6.40 (s, HC_{Ar}, 1H), 6.39 (s, HC_{Ar} , 1H), 6.31 (d, J = 1.3 Hz, HC_{Ar} , 1H), 6.26 (d, J = 1.3 Hz, HC_{Ar} , 4H), 5.98 (s, HC_{Ar} , 1H), 5.79 (s, HC_{Ar} , 1H), 4.16 (br s, $H(CH(Me)NXyl)B(^{Mes}Im)_2$, 2H), 4.12 (q, J = 7.1 Hz, $H(CH(Me)NXyl)B(^{Mes}Im)_2$, 1H), 3.60 (q, J = 6.6 Hz, $H(CH(Me)NXyl)B(^{Mes}Im)_2$, 1H), 2.59 (s, H_3C_{Ar} , 3H), 2.46 (s, H_3C_{Ar} , 3H), 2.38 (s, H_3C_{Ar} , 3H), 2.30 (s, H_3C_{Ar} , 3H), 2.21 (s, H_3C_{Ar} , 3H), 2.19 $(s, H_3C_{Ar}, 6H), 2.18 (s, H_3C_{Ar}, 3H), 2.17 (s, H_3C_{Ar}, 3H), 2.16 (s, H_3C_{Ar}, 3H), 2.10 (s, H_3C_{Ar}, 6H),$ 2.06 (s, H_3C_{Ar} , 3H), 2.00 (s, H_3C_{Ar} , 3H), 1.99 (s, H_3C_{Ar} , 3H), 1.97 (s, H_3C_{Ar} , 6H), 1.91 (s, H_3C_{Ar} , 6H), 1.77 (s, H₃C_{Ar}, 6H), 1.61 (s, H₃C_{Ar}, 3H), 1.55 (s, H₃C_{Ar}, 3H), 1.45 (s, H₃C_{Ar}, 3H), 1.09 (d, J = 7.8 Hz, $H(CH(Me)NXyl)B(^{Mes}Im)_2$, 3H), 1.07 (d, J = 7.8 Hz, $H(CH(Me)NXyl)B(^{Mes}Im)_2$, 3H).

¹H NMR (600 MHz, 373 K, toluene-d8): δ 7.08 (br s, HC_{Ar} , 2H), 6.87 (br t, J = 7.4 Hz, $o-HC_{XVI}$, 1H), 6.80 (t, J = 7.4 Hz, $o-HC_{Xvl}$, 1H), 6.74 (s, HC_{Ar} , 2H), 6.68 (br t, J = 7.4 Hz, $o-HC_{Xvl}$, 1H), 6.65 (br s, HC_{Ar}, 2H), 6.57 (br s, HC_{Ar}, 4H), 6.39 (s, HC_{Ar}, 1H), 6.37 (s, HC_{Ar}, 2H), 5.91 (s, HC_{Ar}, 1H), 4.12 (br s, *H*(CH(Me)NXyl)B(^{Mes}Im)₂, 1H), 3.70 (br q, H(C*H*(Me)NXyl)B(^{Mes}Im)₂, 1H), 2.69 $(s, H_3C_{Ar}, 3H), 2.20 (s, H_3C_{Ar}, 3H), 2.06 (s, H_3C_{Ar}, 3H), 1.96 (s, H_3C_{Ar}, 9H), 1.81 (s, H_3C_{Ar}, 3H),$ 1.71 (br s, H_3C_{Ar} , 3H), 1.65 (s, H_3C_{Ar} , 3H), 1.59 (s, H_3C_{Ar} , 3H), 1.54 (s, H_3C_{Ar} , 6H), 1.44 (br d, J= 5.1 Hz, $H(CH(Me)NXyl)B(^{Mes}Im)_2$, 3H). ¹³C NMR (151 MHz, 298 K, C_6D_6): δ 209.2 (C_{Imid}), 208.3 (C_{Imid}), 201.6, 199.0, 198.0, 196.6, 194.3, 159.3, 155.7, 155.6, 155.4, 154.7, 154.0, 138.6, 138.3, 138.2, 138.1, 138.0, 137.91, 137.87, 137.83, 137.82, 137.7, 137.59, 137.56, 137.5, 137.4, 136.9, 136.6, 136.4, 136.0, 135.9, 135.71, 135.65, 135.5, 135.0, 134.9, 134.02, 133.99, 133.6, 133.4, 132.1, 130.3 (HC_{Ar}), 130.0 (HC_{Ar}), 129.7 (HC_{Ar}), 129.41 (HC_{Ar}), 129.35 (HC_{Ar}), 129.3 (HC_{Ar}) , 129.22 (HC_{Ar}) , 129.19 (HC_{Ar}) , 129.1 (HC_{Ar}) , 129.0 (HC_{Ar}) , 128.5 (HC_{Ar}) , 128.4 (HC_{Ar}) , 127.8 (H C_{Ar}), 127.6 (H C_{Ar}), 127.5 (H C_{Ar}), 127.1 (H C_{Ar}), 126.8 (H C_{Ar}), 126.4 (H C_{Ar}), 125.4 (HC_{Ar}) , 125.2 (HC_{Ar}) , 124.9 (HC_{Ar}) , 124.6 (HC_{Ar}) , 124.5 (HC_{Ar}) , 124.3 (HC_{Ar}) , 124.1 (HC_{Ar}) , 122.9 (H C_{Ar}), 122.4 (H C_{Ar}), 122.3 (H C_{Ar}), 122.19 (H C_{Ar}), 122.15 (H C_{Ar}), 121.8 (H C_{Ar}), 121.7 (HC_{Ar}), 120.7 (HC_{Ar}), 120.5 (HC_{Ar}), 66.0 (H(CH(Me)NXyl)B(^{Mes}Im)₂, overlapping Et₂O peak), 59.9 (H(CH(Me)NXyl)B($^{\text{Mes}}$ Im)₂), 23.0 (H₃C_{Ar}), 22.8 (H₃C_{Ar}), 22.6 (H₃C_{Ar}), 21.04 (H₃C_{Ar}), 20.99 (H_3C_{Ar}) , 20.96 (H_3C_{Ar}) , 20.6 (H_3C_{Ar}) , 20.5 (H_3C_{Ar}) , 20.4 (H_3C_{Ar}) , 20.1 (H_3C_{Ar}) , 19.9 (H_3C_{Ar}) , $19.3C_{Ar}$), 19.68 (H₃C_{Ar}), 19.66 (H₃C_{Ar}), 19.60 (H₃C_{Ar}), 19.57 (H₃C_{Ar}), 19.5 (H₃C_{Ar}), 19.4 (H₃C_{Ar}), 19.31 $(H(CH(Me)NXyl)B(^{Mes}Im)_2)$, 19.28 $H(CH(Me)NXyl)B(^{Mes}Im)_2)$, 19.2 (H_3C_{Ar}) , 19.0 (H_3C_{Ar}) , 18.7 (H_3C_{Ar}) , 18.6 (H_3C_{Ar}) , 18.3 (H_3C_{Ar}) , 18.2 (H_3C_{Ar}) . ¹³C NMR (151 MHz, 373 K, toluene-d8): δ 208.8 (C_{Imid}), 202.63 (C_{Imid}), 172.6, 155.9, 155.7, 138.8, 138.5, 137.3, 137.0, 136.3, 135.1, 134.3, 133.8, 130.7, 130.2, 130.1 (H C_{Ar}), 129.9 (H C_{Ar}), 129.3 (H C_{Ar}), 128.5 (o-H C_{Xyl}),

128.4 (*o*-H*C*_{Xyl}), 126.2 (H*C*_{Ar}), 125.6 (H*C*_{Ar}), 124.9 (*o*-H*C*_{Xyl}), 124.3 (H*C*_{Ar}), 123.7 (H*C*_{Ar}), 122.7 (H*C*_{Ar}), 122.5 (H*C*_{Ar}), 122.2 (H*C*_{Ar}), 61.3 (H(*C*H(Me)NXyl)B(^{Mes}Im)₂), 22.7 (H₃*C*_{Ar}), 21.0 (H₃*C*_{Ar}), 20.97 (H₃*C*_{Ar}), 19.8 (H₃*C*_{Ar}), 19.6 (H₃*C*_{Ar}), 19.5 (H₃*C*_{Ar}), 19.4 (H₃*C*_{Ar}), 19.3 (H₃*C*_{Ar}), 19.0 (H₃*C*_{Ar}), 18.7 (H(CH(*Me*)NXyl)B(^{Mes}Im)₂), 18.3 (H₃*C*_{Ar}). ¹¹B NMR (193 MHz, 298 K, C₆D₆): δ 0.13 (s), -3.02 (s). ¹¹B NMR (193 MHz, 373 K, toluene-*d*8): δ -3.16 (d, J = 100.2 Hz). Anal. Calcd for C₅₁H₅₈BClN₇Ta (**8**): C, 61.48; H, 5.87; N, 9.84. Found: C, 61.72; H, 5.98; N, 9.75. FT-IR (KBr, Nujol, cm⁻¹): ν_{B-H} 2359 (m), 2343 (m); ν_{C=N} 2180 (s). Mp: 167 °C (dec).

Generation of 8 in solution from 6 and 2 eq. xylyl isocyanide. In a 20 mL glass scintillation vial in an inert atmosphere glovebox, compound 6 (14.4 mg, 0.0186 mmol) was dissolved in C₆D₆ (0.25 mL) and the resulting yellow solution was set to stir. In a separate vial, xylyl isocyanide (2 eq., 4.9 mg, 0.0371 mmol) was dissolved in C₆D₆ (0.25 mL) and then the colorless solution was added in one portion to the solution of 6, resulting in an immediate color change to red. The red solution was transferred to a J. Young NMR tube; subsequent ¹H NMR analysis revealed complete and clean conversion to 8, ketenimine 9, and a trace amount of propene. The ¹H NMR spectrum of 8 prepared via this route exactly matched that of isolated 8.

Generation of 8 in solution from 6 and 3 eq. xylyl isocyanide. In a 20 mL glass scintillation vial in an inert atmosphere glovebox, compound 6 (14.4 mg, 0.0186 mmol) was dissolved in C₆D₆ (0.25 mL) and the resulting yellow solution was set to stir. In a separate vial, xylyl isocyanide (3 eq., 7.7 mg, 0.0588 mmol) was dissolved in C₆D₆ (0.25 mL) and then the colorless solution was added in one portion to the solution of 6, resulting in an immediate color change to red. The red solution was transferred to a J. Young NMR tube; subsequent ¹H NMR analysis revealed complete and clean conversion to 8 and ketenimine 9. The ¹H NMR spectrum of 8 prepared via this route exactly matched that of isolated 8.

2,6-Dimethyl-*N*-(**2-methyl-1-propen-1-ylidene**)**benzenamine** (**9**). In an inert atmosphere glovebox, compound **1-Cl** (14.2 mg, 0.0200 mmol) was combined with xylyl isocyanide (4 eq., 10.5 mg, 0.0800 mmol) in a 4 mL glass dram vial. The yellow and white colored solid mixture was dissolved in C_6D_6 (0.25 mL) and the resulting homogeneous, red solution was transferred to a J. Young NMR tube. The tube was sealed and removed from the glovebox. After sitting at room temperature for 1h, 1 H and 13 C NMR analyses indicated that all starting material had been consumed and that **8** and ketenimine **9** had formed. Then, the volatiles were removed under vacuum and the solid mixture was analyzed by LRMS. 1 H NMR (400 MHz, 298 K, C_6D_6): δ 6.92 (m, HC_{Xyl} , 3H), 2.25 (s, H_3C_{Xyl} , 6H), 1.45 (s, (Xyl)N=C=C(Me)₂, 6H). 13 C NMR (101 MHz, 298 K, C_6D_6): δ 206.2 ((Xyl)N=C=C(Me)₂), 137.5 (N- C_{Xyl}), 129.0 (m-H C_{Xyl}), 125.3 (p-C C_{Xyl}), 124.4 (o-H C_{Xyl}), 56.2 ((Xyl)N=C=C(Me)₂), 18.3 (H₃ C_{Xyl}), 15.3 ((Xyl)N=C=C(Me)₂). LRMS (EI) m/z: [M]⁺ calcd for $C_{12}H_{15}$ N (**9**): 173.12; Found: 173.

[H(CH(Me)NXyl)B(MesIm)2]TaCl(OCMe2CMe2O) (10).

Method A. Compound 6 (200 mg, 0.258 mmol) was added to a 50 mL Teflon-sealed tube and dissolved in benzene (15 mL), resulting in a yellow solution. The solution was degassed, and the headspace was refilled with CO. After 2 minutes, the solution changed color from yellow to dark yellow. The flask was sealed, and the solution was stirred vigorously at ambient temperature for 2 days, resulting in an orange solution. Then, the volatiles were removed via lyophilization, yielding an orange-colored powder. The crude product was extracted with Et₂O (2 x 6 mL), and the resulting yellow-orange solution was filtered through Celite, concentrated to a final volume of ca. 0.5 mL, and allowed to sit undisturbed at room temperature for 30 minutes before storing at -40 °C overnight, yielding yellow microcrystals of 10 (34.2 mg, 31% yield). X-ray quality crystals of 10 were grown from a saturated Et₂O solution of 10 at -40 °C. Due to the low yield of material

produced by Method A, characterization was carried out using material obtained from Method B.

The ¹H NMR spectrum of the isolated material made using Method A matched that of analytically pure **10** synthesized by Method B.

Method B. Compound 6 (150 mg, 0.193 mmol) was added to a 50 mL Teflon-sealed tube and dissolved in benzene (6 mL), resulting in a yellow solution, to which excess acetone (3 mL) was added. The solution was degassed, and the headspace was refilled with H₂. The flask was sealed, and the solution was stirred vigorously at ambient temperature for 12 h, resulting in a heterogeneous suspension of fine yellow precipitate in a yellow solution. Then, the volatiles were removed via lyophilization, yielding a yellow powder. The crude product was extracted with toluene (3 x 5 mL), and the resulting yellow solution was filtered through Celite, concentrated to a final volume of ca. 4 mL, and allowed to sit undisturbed at room temperature for 4 hours before storing at -40 °C overnight, yielding yellow microcrystals of **10** (107 mg, 64% yield). ¹H NMR (600 MHz, 298 K, C_6D_6): δ 7.15 (d, J = 1.5 Hz, HC_{Imid} , 1H), 7.12 (d, J = 6.9 Hz, m- HC_{Xyl} , 1H), 7.10 (d, J = 6.9 Hz, $m-HC_{Xyl}$, 1H), 7.05 (d, J = 1.5 Hz, HC_{Imid} , 1H), 6.99 (t, J = 7.4 Hz, $o-HC_{Xyl}$, 1H), 6.81 (s, HC_{Mes} , 1H), 6.78 (s, HC_{Mes} , 1H), 6.76 (s, HC_{Mes} , 2H), 6.27 (d, J = 1.5 Hz, HC_{Imid} , 1H), 6.20 (d, J = 1.5 Hz, HC_{Imid} , 1H), 4.14 (q, J = 6.8 Hz, $H(CH(Me)NXyI)B(^{Mes}Im)_2$, 1H, overlapping $H(CH(Me)NXyl)B(^{Mes}Im)_2$ peak), 4.14 (br s, $H(CH(Me)NXyl)B(^{Mes}Im)_2$, 1H, overlapping $H(CH(Me)NXyl)B(^{Mes}Im)_2$ peak), 2.55 (s, H_3C_{Ar} , 3H), 2.321 (s, H_3C_{Ar} , 3H), 2.315 (s, H_3C_{Ar} , 3H), 2.16 (s, H_3C_{Ar} , 3H), 2.13 (s, H_3C_{Ar} , 3H), 2.12 (s, H_3C_{Ar} , 3H), 2.02 (s, H_3C_{Ar} , 3H), 1.87 $(s, H_3C_{Ar}, 3H), 1.14 (d, J = 7.0 Hz, H(CH(Me)NXyl)B(^{Mes}Im)_2, 3H), 1.12 (s, H_3C_{Pin}, 3H), 0.86 (s, H_3C_{Ar}, 3H), 0.86 (s, H_3C_{Ar},$ H_3C_{Pin} , 3H), 0.76 (s, H_3C_{Pin} , 3H), 0.58 (s, H_3C_{Pin} , 3H). ¹³C NMR (151 MHz, 298 K, C₆D₆): δ 202.0 (C_{Imid}) , 199.3 (C_{Imid}) , 150.7 (C_{Ar}) , 137.7 (C_{Ar}) , 137.6 (C_{Ar}) , 137.2 (C_{Ar}) , 137.14 (C_{Ar}) , 137.08 (C_{Ar}) , 137.06 (C_{Ar}), 136.7 (C_{Ar}), 135.7 (C_{Ar}), 135.5 (C_{Ar}), 134.6 (C_{Ar}), 130.0 (HC_{Mes}), 129.3 (m-HC_{Xyl}),

129.1(HC_{Mes}), 128.9 (HC_{Mes}), 128.6 (*m*-HC_{Xyl}), 128.5 (HC_{Mes}), 125.5 (*o*-HC_{Xyl}), 124.9 (HC_{Imid}), 124.8 (HC_{Imid}), 121.3 (HC_{Imid}), 121.1 (HC_{Imid}), 106.4 (C_{Pin}), 100.4 (C_{Pin}), 59.1 (H(CH(Me)NXyl)B(^{Mes}Im)₂), 28.3 (H₃C_{Pin}), 27.2 (H₃C_{Pin}), 25.7 (H₃C_{Pin}), 21.8 (H₃C_{Ar}), 21.0 (H₃C_{Ar}), 19.8 (H₃C_{Ar}), 19.7 (H₃C_{Ar}), 19.6 (H₃C_{Ar}), 19.3 (H₃C_{Ar}), 19.0 (H₃C_{Ar}), 18.9 (H(CH(*Me*)NXyl)B(^{Mes}Im)₂). ¹¹B NMR (193 MHz, 298 K, C₆D₆): δ –0.40 (s). Anal. Calcd for C₄₀H₅₂BClN₅O₂Ta (**10**): C, 55.73; H, 6.08; N, 8.12. Found: C, 56.04; H, 6.16; N, 7.96. FT-IR (KBr, Nujol, cm⁻¹): ν_{B-H} 2420 (m). Mp: 289 °C (dec).

 $[H(CH(Me)NXyl)B(^{Mes}Im)_2]TaCl(O*CMe_2*CMe_2O)$ (10-*C,*C). Compound 6 (200 mg, 0.258 mmol) was added to a 25 mL Teflon-sealed tube and dissolved in benzene (15 mL), resulting in a yellow solution. The solution was degassed, and the headspace was refilled with ¹³CO. After 2 minutes, the solution changed color from yellow to dark yellow. The flask was sealed, and the solution was stirred vigorously at ambient temperature for 2 days, resulting in an orange solution. Then, the volatiles were removed via lyophilization, yielding an orange colored powder. The crude product was extracted with Et₂O (2 x 4 mL), and the resulting yellow-orange solution was filtered through Celite, concentrated to a final volume of ca. 1.5 mL, and allowed to sit undisturbed at room temperature for 30 minutes before storing at -40 °C overnight, yielding yellow microcrystals of 10-*C,*C (30.4 mg, 27% yield). ¹H NMR (400 MHz, 298 K, C₆D₆): δ 7.15 (d, J = 1.5 Hz, HC_{Imid} , 1H), 7.13 (d, J = 6.9 Hz, $m-HC_{Xvl}$, 1H), 7.09 (d, J = 6.9 Hz, $m-HC_{Xvl}$, 1H), 7.05 (d, J = 1.5Hz, HC_{Imid} , 1H), 6.99 (t, J = 7.4 Hz, $o-HC_{Xvl}$, 1H), 6.81 (s, HC_{Mes} , 1H), 6.79 (s, HC_{Mes} , 1H), 6.76 (s, HC_{Mes} , 2H), 6.26 (d, J = 1.5 Hz, HC_{Imid} , 1H), 6.19 (d, J = 1.5 Hz, HC_{Imid} , 1H), 4.15 (q, J = 6.8Hz, $H(CH(Me)NXyl)B(^{Mes}Im)_2$, 1H, overlapping $H(CH(Me)NXyl)B(^{Mes}Im)_2$ peak), 4.15 (br s, $H(CH(Me)NXyl)B(^{Mes}Im)_2$, 1H, overlapping $H(CH(Me)NXyl)B(^{Mes}Im)_2$ peak), 2.55 (s, H_3C_{Ar} , 3H), 2.321 (s, H₃C_{Ar}, 3H), 2.315 (s, H₃C_{Ar}, 3H), 2.16 (s, H₃C_{Ar}, 3H), 2.13 (s, H₃C_{Ar}, 3H), 2.12 (s,

 H_3C_{Ar} , 3H), 2.02 (s, H_3C_{Ar} , 3H), 1.88 (s, H_3C_{Ar} , 3H), 1.15 (d, J = 6.5 Hz, $H(CH(Me)NXyI)B(^{Mes}Im)_2$, 3H, overlapping H_3C_{Pin} peak), 1.13 (t, $^2J=3.5$ Hz, H_3C_{Pin} , 3H, overlapping H(CH(Me)NXyl)B(MesIm)₂ peak), 0.86 (t, $^2J = 3.5$ Hz, H_3C_{Pin} , 3H), 0.76 (t, $^2J = 3.5$ Hz, H_3 C_{Pin}, 3H), 0.58 (t, 2J = 3.5 Hz, H_3 C_{Pin}, 3H). 13 C NMR (101 MHz, 298 K, C₆D₆, fast scan): δ 106.4 (d, J = 35.4 Hz, * C_{pin}), 100.3 (d, J = 35.4 Hz, * C_{pin}). ¹H-coupled ¹³C NMR (101 MHz, 298) K, C₆D₆): δ 106.4 (dt, J = 35.4 Hz, ${}^2J = 3.0$ Hz, ${}^*C_{\text{pin}}$), 100.3 (dt, J = 35.4 Hz, ${}^2J = 3.0$ Hz, ${}^*C_{\text{pin}}$). **NMR-Monitored Solution** Generation of $[H(CH(Me)NXyl)B(^{Mes}Im)_2]TaCl(O*CMe_2*CMe_2O)$ (10-*C,*C) from 6 and Compound 6 (20.0 mg, 0.026 mmol) was added to a 4 mL glass dram vial and dissolved in C₆D₆ (0.25 mL). The resulting yellow solution was transferred to a J. Young NMR tube and the tube was sealed. Then, the solution was degassed and the headspace was refilled with ¹³CO. The tube was sealed and kept at ambient temperature. ¹³C{¹H} NMR spectra were obtained after 10 minutes, 1 h, 2 h, 4 h, 6 h, 10 h, 24 h, and 48 h. Sequential color changes from yellow to dark yellow to orange were observed over the course of the reaction.

Solution Generation of [H(CH(Me)NXyl)B(MesIm)₂]TaCl(OCMe₂CMe₂O) (10) in the Presence of a Radical Scavenger. In an inert atmosphere glovebox, compound 6 (20.0 mg, 0.026 mmol) and 9,10-dihydroanthracene (5 eq., 23.2 mg, 0.129 mmol) were added to a 4 mL glass dram vial and the solid mixture was dissolved in C₆D₆ (0.25 mL). The solution was transferred to a J. Young NMR tube and the tube was sealed. Then, the solution was degassed and the headspace was refilled with CO. The tube was sealed and kept at ambient temperature for 6 days, resulting in a color change from yellow to orange. ¹H NMR revealed conversion to 10 and several side products after 6 days, with no changes to the resonances for the 9,10-dihydroanthracene protons. ¹H NMR (300 MHz, 298 K, C₆D₆): δ 4.14 (br s, HC_{lmid}, 1H), 7.09 (s, HC_{Anthr}, 140H, 18 eq.), 7.05 (br s,

 HC_{Imid} , 1H), 7.01 (s, HC_{Xyl} , 1H), 6.99 (s, HC_{Xyl} , 1H), 6.96 (br s, HC_{Xyl} , 1H), 6.81 (br s, HC_{Mes} , 1H), 6.70 (br s, HC_{Mes} , 1H), 6.76 (br s, HC_{Mes} , 2H), 6.26 (d, J = 1.7 Hz, HC_{Imid} , 1H), 6.19 (d, J = 1.7 Hz, HC_{Imid} , 1H), 4.16 (q, J = 6.8 Hz, $H(CH(Me)NXyl)B(^{\text{Mes}}Im)_2$, 1H, overlapping $H(CH(Me)NXyl)B(^{\text{Mes}}Im)_2$ peak), 4.16 (br s, $H(CH(Me)NXyl)B(^{\text{Mes}}Im)_2$, 1H, overlapping $H(CH(Me)NXyl)B(^{\text{Mes}}Im)_2$ peak), 3.63 (s, HC_{Anthr} , 80H, 18 eq.), 2.55 (s, H_3C_{Ar} , 3H), 2.33 (s, H_3C_{Ar} , 3H), 2.32 (s, H_3C_{Ar} , 3H), 2.17 (s, H_3C_{Ar} , 3H), 2.13 (s, H_3C_{Ar} , 3H), 2.12 (s, H_3C_{Ar} , 3H), 2.03 (s, H_3C_{Ar} , 3H), 1.88 (s, H_3C_{Ar} , 3H), 1.16 (d, J = 7.0 Hz, $H(CH(Me)NXyl)B(^{\text{Mes}}Im)_2$, 3H), 1.13 (s, H_3C_{Pin} , 3H), 0.86 (s, H_3C_{Pin} , 3H), 0.77 (s, H_3C_{Pin} , 3H), 0.58 (s, H_3C_{Pin} , 3H).

Solution Generation of 1:4:1 mixture of ca. [H(CH(Me)NXyl)B(MesIm)2]TaCl(O*CMe2*CMe2O) (10),[H(CH(Me)NXyl)B(MesIm)2]TaCl(OC(CD3)2C(CH3)2O) $(10-d_6),$ and [H(CH(Me)NXyl)B(MesIm)₂]TaCl(OC(CD₃)₂C(CD₃)₂O) (10-d₁₂) from CO and Acetone-d₆. In an inert atmosphere glovebox, compound 6 (20.0 mg, 0.026 mmol) was added to a 4 mL glass dram vial and dissolved in C_6D_6 (0.25 mL). A stock solution of 1.36 M acetone- d_6 in C_6D_6 (0.5 eq., 9.48 µL, 0.013 mmol) was added to the yellow solution of 6 via micropipette. The solution was quickly transferred to a J. Young NMR tube, and the tube was sealed. Then, the solution was degassed and the headspace was refilled with CO. The tube was sealed and kept at ambient temperature for 24 h, resulting in a color change from yellow to dark yellow. ¹H NMR analysis revealed relatively clean conversion to a 1:4:1 mixture of $10:10-d_0:10-d_{12}$. Then, the volatiles were removed under vacuum, yielding tacky yellow solids. The solids were triturated with hexane (2 x 0.5 mL), resulting in a yellow powder. The yellow powder was dissolved in C₆H₆ (0.25 mL), and toluene- d_8 (2 µL) was added via micropipette to serve as an internal standard. The solution was transferred to a clean J. Young NMR tube and analyzed by ²H NMR spectroscopy. ¹H NMR (600

MHz, 298 K, C_6D_6): δ 7.15 (d, J = 1.4 Hz, HC_{Imid} , 1H), 7.12 (d, J = 7.0 Hz, $m-HC_{Xyl}$, 1H), 7.10 $(d, J = 6.9 \text{ Hz}, m\text{-}HC_{Xvl}, 1H), 7.05 (d, J = 1.4 \text{ Hz}, HC_{Imid}, 1H), 6.98 (t, J = 7.4 \text{ Hz}, o\text{-}HC_{Xvl}, 1H),$ 6.81 (s, HC_{Mes} , 1H), 6.78 (s, HC_{Mes} , 1H), 6.75 (s, HC_{Mes} , 2H), 6.27 (d, J = 1.3 Hz, HC_{Imid} , 1H), 6.20 (J = 1.3 Hz, HC_{Imid} , 1H), 4.14 (q, J = 6.8 Hz, $H(CH(Me)NXyl)B(^{Mes}Im)_2$, 1H, overlapping $H(CH(Me)NXyl)B(^{Mes}Im)_2$ peak), 4.14 (br s, $H(CH(Me)NXyl)B(^{Mes}Im)_2$, 1H, overlapping H(CH(Me)NXyl)B(MesIm)₂ peak), 2.54 (s, H₃C_{Ar}, 3H), 2.32 (s, H₃C_{Ar}, 3H), 2.31 (s, H₃C_{Ar}, 3H), 2.16 (s, H_3C_{Ar} , 3H), 2.13 (s, H_3C_{Ar} , 3H), 2.12 (s, H_3C_{Ar} , 3H), 2.02 (s, H_3C_{Ar} , 3H), 1.87 (s, H_3C_{Ar} , 3H), 1.14 (d, J = 7.0 Hz, H(CH(Me)NXyl)B(MesIm)₂, 3H), 1.122 (s, H_3C_{Pin} of 10, 0.50H relative to the bis(NHC)borate ligand), 1.116 (s, H_3C_{Pin} of 10- d_6 , 1.09H relative to the bis(NHC)borate ligand), 0.860 (s, H_3C_{Pin} of 10, 0.49H relative to the bis(NHC)borate ligand), 0.855 (s, H_3C_{Pin} of $10-d_6$, 1.01H relative to the bis(NHC)borate ligand), 0.763 (s, H_3C_{Pin} of 10, 0.51H relative to the bis(NHC)borate ligand), 0.756 (s, H_3C_{Pin} of $10-d_6$, 1.04H relative to the bis(NHC)borate ligand), 0.579 (s, H_3C_{Pin} of 10, 0.50H relative to the bis(NHC)borate ligand), 0.574 (s, H_3C_{Pin} of 10- d_6 , 1.00H relative to the bis(NHC)borate ligand). ²H NMR (92 MHz, 298 K, C₆H₆): δ 1.08 (br s, D_3C_{Pin} of 10- d_6 , 3D), 0.81 (br s, D_3C_{Pin} of 10- d_6 , 3D), 0.73 (br s, D_3C_{Pin} of 10- d_6 , 3D), 0.55 (br s, D_3 C_{Pin} of 10- d_6 , 3D).

[H(CH(Me)NXyl)B(^{Mes}Im)₂]TaCl(OC(CD₃)₂C(CD₃)₂O) (10-d₁₂). Compound 6 (75.0 mg, 0.0967 mmol) was added to a 25 mL Teflon-sealed tube and dissolved in benzene (2.5 mL), resulting in a yellow solution, to which acetone-d₆ (2.1 eq., 13.0 mg, 14.9 μL, 0.203 mmol) was added via micropipette. The solution was degassed, and the headspace was refilled with H₂. The flask was sealed, and the yellow solution was stirred vigorously at ambient temperature for 2 days, resulting in a homogeneous, dark yellow solution. Then, the volatiles were removed via lyophilization, yielding a brown powder. The crude product was triturated with hexane (2 x 2 mL),

extracted with toluene (2 x 3 mL), and the resulting dark yellow solution was filtered through Celite, concentrated to a final volume of ca. 0.25 mL, and allowed to sit undisturbed at room temperature for 30 min before storing at -40 °C overnight, yielding yellow crystals coated in a tacky brown impurity. The crystals were washed with HMDSO (3 x 0.5 mL) and dried under vacuum, yielding yellow crystals of **10-d**12 (50.3 mg, 60% yield). ¹H NMR (600 MHz, 298 K, C₆D₆): δ 7.15 (d, J = 1.3 Hz, HC_{Imid} , 1H), 7.12 (d, J = 6.9 Hz, m- HC_{Xyl} , 1H), 7.10 (d, 6.9 Hz, m- HC_{Xyl} , 1H), 7.05 (d, J = 1.3 Hz, HC_{Imid} , 1H), 6.99 (t, J = 7.3 Hz, o- HC_{Xyl} , 1H), 6.81 (s, HC_{Mes} , 1H), 6.78 (s, HC_{Mes} , 1H), 6.76 (s, HC_{Mes} , 2H), 6.27 (s, J = 1.2 Hz, HC_{Imid} , 1H), 6.20 (s, J = 1.2 Hz, HC_{Imid} , 1H), 4.14 (q, J = 6.7 Hz, $H(CH(Me)NXyl)B(^{Mes}Im)_2$, 1H, overlapping $H(CH(Me)NXyl)B(^{Mes}Im)_2$ peak), 4.14 (br s, $H(CH(Me)NXyl)B(^{Mes}Im)_2$, 1H, overlapping $H(CH(Me)NXyl)B(^{Mes}Im)_2$ peak), 2.55 (s, H_3C_{Ar} , 3H), 2.321 (s, H_3C_{Ar} , 3H), 2.315 (s, H_3C_{Ar} , 3H), 2.16 (s, H_3C_{Ar} , 3H), 2.13 (s, H_3C_{Ar} , 3H), 2.12 (s, H_3C_{Ar} , 3H), 2.02 (s, H_3C_{Ar} , 3H), 1.87 (s, H_3C_{Ar} , 3H), 1.14 (d, J = 7.0 Hz, $H(CH(Me)NXyl)B(^{Mes}Im)_2$, 3H). ²H NMR (92 MHz, 298 K, C₆H₆): δ 1.07 (br s, D_3C_{Pin} , 3D), 0.79 (br s, D_3C_{Pin} , 3D), 0.72 (br s, D_3C_{Pin} , 3D), 0.54 (br s, D_3C_{Pin} , 3D).

NMR-Monitored Scrambling Experiment between $[H(CH(Me)NXyl)B(^{Mes}Im)_2]TaCl(OCMe_2CMe_2O)$ (10) and $[H(CH(Me)NXyl)B(^{Mes}Im)_2]TaCl(OC(CD_3)_2C(CD_3)_2O)$ (10- d_{12}). In an inert atmosphere glovebox, compound 10 (7.0 mg, 0.008 mmol) was combined with compound 10- d_{12} (7.0 mg, 0.008 mmol) in a 4 mL glass dram vial. The solid mixture was dissolved in C_6D_6 (0.25 mL), and the resulting yellow solution was transferred to a J. Young NMR tube. The tube was sealed and a 1H NMR spectrum was obtained. Then, the tube was heated to 80 °C for 2 days. 1H NMR analysis revealed no scrambling of deuterium atoms between 10 and 10- d_{12} under these conditions. 1H NMR of 1:1 10:10- d_{12} (400 MHz, 298 K, C_6D_6): δ 7.15 (d, J = 1.4 Hz, HC_{Imid} , 1H), 7.11 (m, m-

 HC_{Xyl} , 2H), 7.05 (d, J = 1.4 Hz, HC_{Imid} , 1H), 6.99 (t, J = 7.4 Hz, o- HC_{Xyl} , 1H), 6.81 (s, HC_{Mes} , 1H), 6.79 (s, HC_{Mes} , 1H), 6.76 (s, HC_{Mes} , 2H), 6.26 (d, J = 1.4 Hz, HC_{Imid} , 1H), 6.19 (d, J = 1.4 Hz, HC_{Imid} , 1H), 4.15 (q, J = 7.0 Hz, $H(CH(Me)NXyl)B(^{Mes}Im)_2$, 1H, overlapping $H(CH(Me)NXyl)B(^{Mes}Im)_2$ peak), 4.15 (br s, $H(CH(Me)NXyl)B(^{Mes}Im)_2$, 1H, overlapping $H(CH(Me)NXyl)B(^{Mes}Im)_2$ peak), 2.55 (s, H_3C_{Ar} , 3H), 2.324 (s, H_3C_{Ar} , 3H), 2.319 (s, H_3C_{Ar} , 3H), 2.16 (s, H_3C_{Ar} , 3H), 2.13 (s, H_3C_{Ar} , 3H), 2.12 (s, H_3C_{Ar} , 3H), 2.03 (s, H_3C_{Ar} , 3H), 1.88 (s, H_3C_{Ar} , 3H), 1.15 (d, J = 6.8 Hz, $H(CH(Me)NXyl)B(^{Mes}Im)_2$, 3H), 1.13 (s, H_3C_{Pin} of 10, 1.5H relative to the bis(NHC)borate ligand), 0.86 (s, H_3C_{Pin} of 10, 1.5H relative to the bis(NHC)borate ligand), 0.58 (s, H_3C_{Pin} of 10, 1.5H relative to the bis(NHC)borate ligand).

Synthesis of a ca. 1:2:1 mixture of [H(CH(Me)NXyl)B(MesIm)2]TaCl(OCMe2CMe2O) (10), [H(CH(Me)NXyl)B(MesIm)2]TaCl(OC(CD3)2C(CH3)2O) (10- d_6), and [H(CH(Me)NXyl)B(MesIm)2]TaCl(OC(CD3)2C(CD3)2O) (10- d_{12}) from H2, Acetone, and Acetone- d_6 . Compound 6 (75.0 mg, 0.0967 mmol) was added to a 50 mL Teflon-sealed tube and dissolved in benzene (3 mL), resulting in a yellow solution, to which excess 1:1 acetone:acetone- d_6 (0.25 mL each) was added. The solution was degassed, and the headspace was refilled with H2. The flask was sealed, and the solution was stirred vigorously at ambient temperature for 5 h, resulting in a homogeneous, yellow solution. Then, the volatiles were removed via lyophilization, yielding a yellow powder. The crude product was extracted with toluene (2 x 4 mL), and the resulting yellow solution was filtered through Celite, concentrated to a final volume of ca. 1 mL, and allowed to sit undisturbed at room temperature for 20 minutes before storing at -40 °C overnight, yielding yellow microcrystals of 10, 10- d_6 , and 10- d_{12} (41.4 mg, 49% yield, ca. 1:2:1 ratio). 1 H NMR (600 MHz, 298 K, C_6D_6): δ 7.15 (d, J = 1.4 Hz, HC_{Imid} , 1H), 7.12 (d, J = 7.0 Hz,

 $m-HC_{Xyl}$, 1H), 7.10 (d, J = 6.9 Hz, $m-HC_{Xyl}$, 1H), 7.05 (d, J = 1.4 Hz, HC_{Imid} , 1H), 6.98 (t, J = 7.4Hz, $o-HC_{Xyl}$, 1H), 6.81 (s, HC_{Mes} , 1H), 6.78 (s, HC_{Mes} , 1H), 6.76 (s, HC_{Mes} , 2H), 6.27 (d, J = 1.3Hz, HC_{Imid} , 1H), 6.20 (J = 1.3 Hz, HC_{Imid} , 1H), 4.14 (q, J = 6.8 Hz, $H(CH(Me)NXyI)B(^{Mes}Im)_2$, 1H, overlapping $H(CH(Me)NXyl)B(^{Mes}Im)_2$ peak), 4.14 (br s, $H(CH(Me)NXyl)B(^{Mes}Im)_2$, 1H, overlapping $H(CH(Me)NXyl)B(^{Mes}Im)_2$ peak), 2.54 (s, H_3C_{Ar} , 3H), 2.32 (s, H_3C_{Ar} , 3H), 2.31 (s, H_3C_{Ar} , 3H), 2.16 (s, H_3C_{Ar} , 3H), 2.13 (s, H_3C_{Ar} , 3H), 2.12 (s, H_3C_{Ar} , 3H), 2.02 (s, H_3C_{Ar} , 3H), 1.87 (s, H_3C_{Ar} , 3H), 1.14 (d, J = 7.0 Hz, H(CH(Me)NXyl)B(^{Mes}Im)₂, 3H), 1.123 (s, H_3C_{Pin} of 10, 0.77H relative to the bis(NHC)borate ligand), 1.118 (s, H_3C_{Pin} of 10- d_6 , 0.73H relative to the bis(NHC)borate ligand), 0.861 (s, H₃C_{Pin} of 10, 0.76H relative to the bis(NHC)borate ligand), 0.856 (s, H_3C_{Pin} of 10- d_6 , 0.71H relative to the bis(NHC)borate ligand), 0.764 (s, H_3C_{Pin} of 10, 0.76H relative to the bis(NHC)borate ligand), 0.757 (s, H₃C_{Pin} of 10-d₆, 0.70H relative to the bis(NHC)borate ligand), 0.580 (s, H_3C_{Pin} of 10, 0.77H relative to the bis(NHC)borate ligand), 0.575 (s, H_3C_{Pin} of $10-d_6$, 0.70H relative to the bis(NHC)borate ligand). ²H NMR (92 MHz, 298 K, C_6H_6): δ 1.08 (br s, D_3C_{Pin} , 3D), 0.79 (br s, D_3C_{Pin} , 3D), 0.73 (br s, D_3C_{Pin} , 3D), 0.53 (br s, D_3C_{Pin} , 3D).

[H(CH(Me)NXyl)B(MesIm)2]TaCl(OCEt2CEt2O) (11). Compound 6 (200 mg, 0.258 mmol) was added to a 50 mL Teflon-sealed tube and dissolved in benzene (6 mL), resulting in a yellow solution, to which excess 3-pentanone (2 mL) was added. The solution was degassed, and the headspace was refilled with H₂. The flask was sealed, and the solution was stirred vigorously at ambient temperature for 5 h, resulting in a bright yellow solution. Then, the volatiles were removed via lyophilization, yielding a yellow powder. The crude product was extracted with toluene (2 x 4 mL), and the resulting yellow solution was filtered through Celite, concentrated to a final volume of ca. 2 mL, and allowed to sit undisturbed at room temperature for 30 min before storing at –40

°C overnight, yielding yellow microcrystals of 11 (151 mg, 64% yield). ¹H NMR (600 MHz, 298 K, C_6D_6): 7.18 (d, J = 1.5 Hz, HC_{Imid} , 1H), 7.15 (d, J = 8.0 Hz, $m-HC_{Xvl}$, 1H), 7.11 (d, J = 8.0 Hz, $m-HC_{Xyl}$, 1H), 7.04 (d, J = 1.5 Hz, HC_{Imid} , 1H), 6.99 (t, J = 7.6 Hz, $o-HC_{Xyl}$, 1H), 6.80 (s, HC_{Mes} , 1H), 6.79 (s, HC_{Mes} , 2H), 6.76 (s, HC_{Mes} , 1H), 6.23 (d, J = 1.5 Hz, HC_{Imid} , 1H), 6.20 (d, J = 1.5Hz, HC_{Imid} , 1H), 4.20 (q, J = 6.8 Hz, $H(CH(Me)NXyl)B(^{Mes}Im)_2$, 1H, overlapping H(CH(Me)NXyl)B(MesIm)₂ peak), 4.20 (br s, H(CH(Me)NXyl)B(MesIm)₂, 1H, overlapping $H(CH(Me)NXyl)B(^{Mes}Im)_2 peak)$, 2.76 (sx, J = 7.0 Hz, H_2C_{Diol} , 1H), 2.56 (s, H_3C_{Ar} , 3H), 2.36 (s, H_3C_{Ar} , 3H), 2.234 (s, H_3C_{Ar} , 3H), 2.226 (s, H_3C_{Ar} , 3H), 2.17 (s, H_3C_{Ar} , 3H), 2.14 (s, H_3C_{Ar} , 3H), 2.10 (s, H_3C_{Ar} , 3H), 1.94 (s, H_3C_{Ar} , 3H), 1.59 (sx, J = 7.5 Hz, H_2C_{Diol} , 1H), 1.54 (sx, J = 7.0 Hz, H_2C_{Diol} , 1H), 1.41 (sx, J = 7.9 Hz, H_2C_{Diol} , 1H), 1.16 (sx, J = 7.0 Hz, H_2C_{Diol} , 1H), 1.14 (sx, J = 7.0 Hz, H_2C_{Diol} , 1H), 1.15 (sx, J = 7.0 Hz, H_2C_{Diol} , 1H), 1.16 (sx, J = 7.0 Hz, H_2C_{Diol} , 1H), 1.17 (sx, J = 7.0 Hz, H_2C_{Diol} , 1H), 1.18 (sx, J = 7.0 Hz, H_2C_{Diol} , 1H), 1.19 (sx, J = 7.0 Hz, H_2C_{Diol} , 1H), 1.19 (sx, J = 7.0 Hz, H_2C_{Diol} , 1H), 1.19 (sx, J = 7.0 Hz, H_2C_{Diol} , 1H), 1.19 (sx, J = 7.0 Hz, H_2C_{Diol} , 1H), 1.19 (sx, J = 7.0 Hz, H_2C_{Diol} , 1H), 1.10 (sx, J = 7.0 Hz, H_2C_{Diol} , 1H), 1.11 (sx, J = 7.0 Hz, H_2C_{Diol} , 1H), 1.12 (sx, J = 7.0 Hz, H_2C_{Diol} , 1H), 1.14 (sx, J = 7.0 Hz, H_2C_{Diol} , 1H), 1.15 (sx, J = 7.0 Hz, H_2C_{Diol} , 1H), 1.16 (sx, J = 7.0 Hz, H_2C_{Diol} , 1H), 1.17 (sx, J = 7.0 Hz, H_2C_{Diol} , 1H), 1.18 (sx, J = 7.0 Hz, H_2C_{Diol} , 1H), 1.19 (sx, J = 7.0 Hz, H_2C_{Diol} , 1H), 1.19 (sx, J = 7.0 Hz, H_2C_{Diol} , 1H), 1.11 (sx, J = 7.0 Hz, H_2C_{Diol} , 1H), 1.11 (sx, J = 7.0 Hz, H_2C_{Diol} , 1H), 1.12 (sx, J = 7.0 Hz, H_2C_{Diol} , 1H), 1.12 (sx, J = 7.0 Hz, H_2C_{Diol} , 1H), 1.14 (sx, J = 7.0 Hz, H_2C_{Diol} , 1H), 1.15 (sx, J = 7.0 Hz, H_2C_{Diol} , 1H), 1.16 (sx, J = 7.0 Hz, H_2C_{Diol} , 1H), 1.17 (sx, J = 7.0 Hz, H_2C_{Diol} , 1H), 1.18 (sx, J = 7.0 Hz, H_2C_{Diol} , 1H), 1.19 (sx, J = 7.0 Hz, H_2C_{Diol} , 1H), 1.10 (sx, J = 7.0 Hz, H_2C_{Diol} , 1H), 1.11 (sx, J = 7.0 Hz, H_2C_{Diol} , 1H), 1.12 (sx, J = 7.0 Hz, H_2C_{Diol} , 1H), 1.14 (sx, J = 7.0 Hz, H_2C_{Diol} , 1H), 1.15 (sx, J = 7.0 Hz, H_2C_{Diol} , 1H), 1.15 (sx, J = 7.0 Hz, H_2C_{Diol} , 1H), 1.15 (sx, J = 7.0 Hz, H_2C_{Diol} , 1H), 1.15 (sx, J = 7.0 Hz, H_2C_{Diol} , 1H), 1.15 (sx, J = 7.0 Hz, H_2C_{Diol} , 1H), 1.15 (sx, J = 7.0 Hz, H_2C_{Diol} , 1H), 1.15 (sx, J = 7.0 Hz, H_2C_{Diol} , 1H), 1.15 (sx, J = 7.0 Hz, H_2C_{Diol} , 1H), 1.15 (sx, J = 7.0 Hz, H_2C_{Diol} , 1H), 1.15 (sx, J = 7.0 Hz, H_2C_{Diol} , 1H), 1 7.6 Hz, H_2C_{Diol} , 1H), 1.10 (d, J = 6.7 Hz, $H(CH(Me)NXyl)B(^{Mes}Im)_2$, 3H), 1.07 (sx, J = 7.0 Hz, H_2C_{Diol} , 1H), 0.64 (t, J = 7.1 Hz, H_3C_{Diol} , 3H), 0.56 (t, J = 7.6 Hz, H_3C_{Diol} , 3H), 0.49 (t, J = 7.6 Hz, H_3C_{Diol} , 3H), 0.38 (sx, J = 7.4 Hz, H_2C_{Diol} , 1H), 0.21 (t, J = 7.3 Hz, H_3C_{Diol} , 3H). ¹³C NMR (151) MHz, 298 K, C₆D₆): δ 201.8 (C_{Imid}), 200.4 (C_{Imid}), 150.9 (C_{Ar}), 137.8 (C_{Ar}), 137.7 (C_{Ar}), 137.2 (C_{Ar}) , 137.1 (C_{Ar}) , 137.01 (C_{Ar}) , 136.99 (C_{Ar}) , 136.88 (C_{Ar}) , 135.32 (C_{Ar}) , 135.29 (C_{Ar}) , 135.0 (C_{Ar}) , 130.3 $(m-HC_{XyI})$, 129.34 (HC_{Mes}) , 129.29 (HC_{Mes}) , 129.0 (HC_{Mes}) , 128.9 (HC_{Mes}) , 125.7 $(m-HC_{Mes})$ HC_{Xyl}), 125.4 (o- HC_{Xyl}), 125.1 (HC_{Imid}), 125.0 (HC_{Imid}), 121.3 (HC_{Imid}), 121.1 (HC_{Imid}), 113.5 (C_{Diol}) , 109.3 (C_{Diol}) , 58.0 $(H(CH(\text{Me})\text{NXyl})B(^{\text{Mes}}\text{Im})_2)$, 27.2 (H_2C_{Diol}) , 26.5 (H_2C_{Diol}) , 26.1 (H_2C_{Diol}) , 23.3 (H_2C_{Diol}) , 21.9 (H_3C_{Ar}) , 21.03 (H_3C_{Ar}) , 20.96 (H_3C_{Ar}) , 20.2 (H_3C_{Ar}) , 20.0 (H_3C_{Ar}) , 19.70 (H₃ C_{Ar}), 19.66 (H₃ C_{Ar}), 19.1 (H₃ C_{Ar}), 18.5 (H(CH(Me)NXyl)B(MesIm)₂), 10.4 (H₃ C_{Diol}), 10.2 (H₃ C_{Diol}), 10.0 (H₃ C_{Diol}), 8.1 (H₃ C_{Diol}). ¹¹B NMR (193 MHz, 298 K, C₆D₆): δ –0.70 (s). Anal. Calcd for C₄₄H₅₉BClN₅O₂Ta (11): C, 57.62; H, 6.48; N, 7.64. Found: C, 57.85; H, 6.48; N, 7.65. FT-IR (KBr, Nujol, cm⁻¹): v_{B-H} 2414 (m). Mp: 260 °C (dec).

ASSOCIATED CONTENT

Supporting Information. The following files are available free of charge. NMR spectra, IR absorbance spectra, and crystallographic information (PDF).

Accession Codes. CCDC 2073577–2073585 contain the supplementary crystallographic data for this paper. These data can be obtained free of charge via www.ccdc.cam.ac.uk/data_request/cif, or by emailing data_request@ccdc.cam.ac.uk, or by contacting The Cambridge Crystallographic Data Centre, 12 Union Road, Cambridge CB2 1EZ, UK; fax: +44 1223 336033.

AUTHOR INFORMATION

Corresponding Author

*John Arnold - Department of Chemistry, University of California, Berkeley, California 94720, United States; Email: arnold@berkeley.edu

Notes

The authors declare no competing financial interest.

ACKNOWLEDGMENT

This research was funded by the NSF (Grant No. CHE-1465188 and 1954612 to J.A. and R.G.B.). J.I.F. and M.A.B. acknowledge support from NSF graduate research fellowships (Grant No. DGE 1752814 and 1106400, respectively). Instruments in CoC-NMR (UC Berkeley) are supported in part by NIH S10OD024998. We thank Dr. Nicholas S. Settineri of the CHEXRAY X-ray crystallographic facility for crystallographic assistance. We thank Dr. Zhongrui Zhou of the

QB3 Mass Spectrometry facility for assistance with mass spectrometry experiments. We thank Erik T. Ouellette, I. Joseph Brackbill, Dr. Trevor D. Lohrey, and Anukta Jain for helpful discussions.

REFERENCES

- (1) Schulz, H. Short History and Present Trends of Fischer-Tropsch Synthesis. *Appl. Catal. A: Gen.* **1999**, *186*, 3–12.
- (2) Dekleva, T. W.; Forster, D. Mechanistic Aspects of Transition-Metal-Catalyzed Alcohol Carbonylations. In *Advances in Catalysis*, Vol. 34; 1986; pp 81–130.
- (3) Jones, J. H. The CativaTM Process for the Manufacture of Acetic Acid: Iridium Catalyst Improves Productivity in an Established Industrial Process. *Platin. Met. Rev.* **2000**, *44*, 94–105.
- (4) Beller, M.; Cornils, B.; Frohning, C. D.; Kohlpaintner, C. W. Progress in Hydroformylation and Carbonylation. *J. Mol. Catal. A* **1995**, *104*, 17–85.
- (5) Hartwig, J. F. Organotransition Metal Chemistry, from Bonding to Catalysis; University Science Books, 2010.
- (6) Durfee, L. D.; Rothwell, I. P. Chemistry of η^2 -Acyl, η^2 -Iminoacyl, and Related Functional Groups. *Chem. Rev.* **1988**, *88*, 1059–1079.
- (7) Kuhlmann, E. J.; Alexander, J. J. Carbon Monoxide Insertion into Transition Metal-Carbon Sigma-Bonds. *Coord. Chem. Rev.* **1980**, *33*, 195–225.
- (8) Alexander, J. J. Insertions into Transition Metal-Carbon Bonds. In *The Chemistry of the Metal Carbon Bond, Volume 2: The Nature and Cleavage of Metal-Carbon Bonds*; Hartley, F. R., Patai, S., Eds.; John Wiley & Sons Ltd, 1985; pp 339–400.

- (9) Schrock, R. R.; Parshall, G. W. σ-Alkyl and -Aryl Complexes of the Group 4-7 Transition Metals. *Chem. Rev.* **1976**, *76*, 243–268.
- (10) Tomson, N. C.; Yan, A.; Arnold, J.; Bergman, R. G. An Unusally Diverse Array of Products Formed upon Carbonylation of a Dialkylniobium Complex. *J. Am. Chem. Soc.* **2008**, *130*, 11262–11263.
- (11) Dawson, D. Y.; Arnold, J. Organotantalum Bis(Amidinate) Complexes: Synthesis and Characterization of Methyl, Methylidene, Benzyl, and Imido Derivatives. *Organometallics* **1997**, *16*, 1111–1113.
- (12) Gómez, M.; Gómez-Sal, P.; Jiménez, G.; Martín, A.; Royo, P.; Sánchez-Nieves, J. Insertion of CO and CNR into Tantalum-Methyl Bonds of Imido(pentamethylcyclopentadienyl)tantalum Complexes. X-Ray Crystal Structures of $[TaCp*(NR)-Me\{\eta^2-C(Me)=NR\}]$ and $[TaCp*Cl(O)\{\eta^2-C(Me)=NR\}]$ ($R=2,6-Me_2C_6H_3$). Organometallics 1996, 15, 3579–3587.
- (13) Wood, C. D.; Schrock, R. R. Reaction of CO with Ta(η⁵-C₅Me₅)Me₄. Intramolecular Reductive Coupling of Carbon Monoxide via an "η²-Acetone" Intermediate. *J. Am. Chem. Soc.* **1979**, *101*, 5421–5422.
- (14) Conde, A.; Fandos, R.; Otero, A.; Rodríguez, A.; Terreros, P. Synthesis and Reactivity of Monocyclopentadienyltantalum(V) Siloxide Complexes. *Eur. J. Inorg. Chem.* **2008**, *19*, 3062–3067.

- (15) Meinhart, J. D.; Santarsiero, B. D; Grubbs, R. H. Carbonylation of Titanocene Cyclobutenes. Synthesis and Characterization of a Titanocene-Vinylketene Complex. *J. Am. Chem. Soc.* **1986**, *108*, 3318–3323.
- (16) Gómez, M. (Alkyl)(monocyclopentadienyl)niobium and -tantalum Complexes in Insertion Processes. *Eur. J. Inorg. Chem.* **2003**, *20*, 3681–3697.
- (17) Kepp, K. P. A Quantitative Scale of Oxophilicity and Thiophilicity. *Inorg. Chem.* **2016**, 55, 9461–9470.
- (18) Greenwood, N. N.; Earnshaw, A. *Chemistry of the Elements*, 2nd ed.; Butterworth-Heinemann, 1997.
- (19) Gianetti, T. L.; Tomson, N. C.; Arnold, J.; Bergman, R. G. Z-Selective, Catalytic Internal Alkyne Semihydrogenation under H₂/CO Mixtures by a Niobium(III) Imido Complex. *J. Am. Chem. Soc.* **2011**, *133*, 14904–14907.
- (20) Garner, M. E.; Hohloch, S.; Maron, L.; Arnold, J. A New Supporting Ligand in Actinide Chemistry Leads to Reactive Bis(NHC)Borate-Supported Thorium Complexes. *Organometallics* **2016**, *35*, 2915–2922.
- (21) Ziegler, J. A.; Prange, C.; Lohrey, T. D.; Bergman, R. G.; Arnold, J. Hydroboration Reactivity of Niobium Bis(N-heterocyclic carbene)borate Complexes. *Inorg. Chem.* **2018**, *57*, 5213–5224.
- (22) Bellemin-Laponnaz, S.; Dagorne, S. Group 1 and 2 and Early Transition Metal Complexes Bearing N-heterocyclic Carbene Ligands: Coordination Chemistry, Reactivity, and Applications. *Chem. Rev.* **2014**, *114*, 8747–8774.

- (23) Romain, C.; Bellemin-laponnaz, S.; Dagorne, S. Recent progress on NHC-stabilized early transition metal (group 3–7) complexes: Synthesis and applications. *Coord. Chem. Rev.* **2020**, *422*, 213411-213442.
- (24) Gade, L. H.; Bellemin-Laponnaz, S. Chiral N-Heterocyclic Carbenes as Stereodirecting Ligands in Asymmetric Catalysis. *Top. Organomet. Chem.* **2006**, *21*, 117–157.
- (25) Campeau, L. C.; Hazari, N. Cross-Coupling and Related Reactions: Connecting Past Success to the Development of New Reactions for the Future. *Organometallics* **2019**, *38*, 3–35.
- (26) Bedford, R. B.; Betham, M.; Bruce, D. W.; Davis, S. A.; Frost, R. M.; Hird, M. Iron Nanoparticles in the Coupling of Alkyl Halides with Aryl Grignard Reagents. *Chem. Commun.* **2006**, *219*, 1398–1400.
- (27) Bourissou, D.; Guerret, O.; Gabbaï, F. P.; Bertrand, G. Stable Carbenes. *Chem. Rev.* **2000**, 100, 39–91.
- (28) Fostvedt, J. I.; Lohrey, T. D.; Bergman, R. G.; Arnold, J. Structural Diversity in Multinuclear Tantalum Polyhydrides Formed via Reductive Hydrogenolysis of Metal-Carbon Bonds. *Chem. Commun.* **2019**, *55*, 13263–13266.
- (29) Tomson, N. C.; Arnold, J.; Bergman, R. G. Synthesis, Characterization, and Reactions of Isolable (β-diketiminato)niobium(III) Imido Complexes. *Organometallics* **2010**, *29*, 5010–5025.
- (30) Guiducci, A. E.; Cowley, A. R.; Skinner, M. E. G.; Mountford, P. Novel Double Substrate Insertion versus Isocyanate Extrusion in Reactions of Imidotitanium Complexes with CO₂: Critical Dependence on Imido N-Substituents. *J. Chem. Soc.*, *Dalton Trans.* **2001**, 1392–1394.

- (31) Bannister, R. D.; Levason, W.; Light, M. E.; Reid, G.; Zhang, W. Complexes of TaOCl₃ and TaSCl₃ with Neutral N- and O-Donor Ligands Synthesis, Properties and Comparison with the Niobium Analogues. *Polyhedron* **2019**, *167*, 1–10.
- (32) Tayebani, M.; Kasani, A.; Feghali, K.; Gambarotta, S.; Bensimon, C. The reduction of Nb₂Cl₆(tmeda)₂ by R₂NLi. Formation of a diamagnetic niobium(II) cluster with short Nb–Nb triple bond and amide C–N bond cleavage. *Chem. Commun.* **1997**, 2001–2002.
- (33) Goux, J.; Le Gendre, P.; Richard, P.; Moïse, C. Oxo and Hydroxo Tantalocene Complexes: Synthesis and Reactivity. X-ray Molecular Structures of $[(\eta^5-Cp^*)TaCl(OH)(\eta^5-C_5H_4SiMe_3)]^+Cl^-$, $[(\eta^5-Cp^*)TaCl(=O)(\eta^5-C_5H_4SiMe_3)]$, and $[(\eta^5-Cp^*)TaCl_2(\eta^5-C_5H_4SiMe_3)]^+PF_6^-$. Organometallics **2005**, 24, 4902–4907.
- (34) Mullins, S. M.; Bergman, R. G.; Arnold, J. Double Group Transfer Reactions of an Unsaturated Tantalum Methylidene Complex with Pyridine *N*-Oxides. *Organometallics* **1999**, *18*, 4465-4467.
- (35) Parkin, G.; Whinnery, L. R.; van Asselt, A.; Leahy, D. J.; Hua, N. G.; Quan, R. W.; Henling, L. M.; Schaefer, W. P.; Santarsiero, B. D.; Bercaw, J. E. Oxo-Hydrido and Imido-Hydrido Derivatives of Permethyltantalocene. Structures of (η⁵-C₅Me₅)₂Ta(=O)H and (η⁵-C₅Me₅)₂Ta(=NC₆H₅)H: Doubly or Triply Bonded Tantalum Oxo and Imido Ligands? *Inorg. Chem.* **1992**, *31*, 82–85.
- (36) Horrillo-Martinez, P.; Patrick, B. O.; Schafer, L. L.; Fryzuk, M. D. Oxygen extrusion from amidate ligands to generate terminal Ta=O units under reducing conditions. How to successfully use amidate ligands in dinitrogen coordination chemistry. *Dalton Trans.* **2012**, *41*, 1609–1616.

- (37) Anderson, L. L.; Schmidt, J. A. R.; Arnold, J.; Bergman, R. G. Neutral and Cationic Alkyl Tantalum Imido Complexes: Synthesis and Migratory Insertion Reactions. *Organometallics* **2006**, *25*, 3394–3406.
- (38) Burckhardt, U.; Casty, G. L.; Gavenonis, J.; Tilley, T. D. Neutral and Anionic Silyl Hydride Derivatives of the Tantalum Imido Fragment Cp*(DippN=)Ta (Cp*=η⁵-C₅Me₅; Dipp=2,6-ⁱPr₂C₆H₃). Reactive σ-Bonds and Intramolecular C-H Bond Activations Involving the Silyl Ligands. *Organometallics* **2002**, *21*, 3108–3122.
- (39) Gavenonis, J.; Tilley, T. D. Tantalum Alkyl and Silyl Complexes of the Bulky (Terphenyl)Imido Ligand [2,6-(2,4,6-Me₃C₆H₂)₂C₆H₃N=]²⁻ ([Ar*N=]²⁻). Generation and Reactivity of [(Ar*N=)(Ar*NH)Ta(H)(OSO₂CF₃)], Which Reversibly Transfers Hydride to an Aromatic Ring of the Arylamide Ligand. *Organometallics* **2002**, *21*, 5549–5563.
- (40) Burckhardt, U.; Tilley, T. D. Carbonylation Chemistry of the Tantalum Silyl Hydride Cp*(2,6- ⁱPr₂C₆H₃N=)Ta[Si(SiMe₃)₃]H: The Unexpected Formation of a Ta(V) Carbonyl Complex and the Complete Reduction of CO. *J. Am. Chem. Soc.* **1999**, *121*, 6328–6329.
- (41) Soo, H. S.; Diaconescu, P. L.; Cummins, C. C. A Sterically Demanding Enolate Ligand: Tantalum Ligation and Pyridine Coupling. *Organometallics* **2004**, *23*, 498-503.
- (42) Chamberlain, L. R.; Rothwell, I. P.; Huffman, J. C. Reactivity of Tantalum η^2 -Iminoacyl Groups: Intramolecular Coupling, Reduction, and Dealkylation. *J. Chem. Soc., Chem. Commun.* **1986**, 1203–1205.

- (43) Galakhov, M. V.; Gómez, M.; Jiménez, G.; Royo, P. Synthesis and Dynamic Behavior of (Pentamethylcyclopentadienyl)Azatantalacyclopropane Complexes. Crystal Structures of TaCp*Cl₄[C(Me)(NHR)] and TaCp*Me₂(η²-Me₂CNR). *Organometallics* **1995**, *14*, 1901–1910.
- (44) Galakhov, M. V.; Gómez, M.; Jiménez, G.; Royo, P.; Pellinghelli, M. A.; Tiripicchio, A. Insertion of Isocyanides into Tantalum-Carbon Bonds of Azatantalacyclopropane Complexes. Crystal Structures of $TaCp*Cl_3(\eta^2-NRCMe_2CNHR)$, $TaCp*Me(NR)(NRCMe=CMe_2)$, and $TaCp*Me(NR)(\eta^2-NR=CCMe_2CMe=NR)$ ($R=2,6-Me_2C_6H_3$). Organometallics 1995, 14, 2843–2854.
- (45) Xiang, L.; Xie, Z. Reaction of $[\eta^1:\eta^5-(R_2NCH_2CH_2)C_2B_9H_{10}]$ TaMe₃ with Isonitriles: Effects of Nitrogen Substituents on Product Formation. *Organometallics* **2016**, *35*, 1430–1439.
- (46) Planalp, R. P.; Andersen, R. A. Cleavage of Carbon Monoxide by Mononuclear Zirconium Dialkyls: Formation of a (μ-Oxo)dialkyl and an Enolate. *J. Am. Chem. Soc.* **1983**, *105*, 7774–7775.
- (47) Andersen, R. A. Dialkylbis[bis(trimethylsilyl)amido]zirconium(IV) and -hafnium(IV). Preparation and Reaction with Carbon Dioxide and *tert*-Butyl Isocyanide. *Inorg. Chem.* **1979**, *18*, 2928–2932.
- (48) Wolczanski, P. T.; Bercaw, J. E. On the Mechanisms of Carbon Monoxide Reduction with Zirconium Hydrides. *Acc. Chem. Res.* **1980**, *13*, 121–127.
- (49) Wolczanski, P. T.; Bercaw, J. E. Dihydrogen Reduction of Isocyanides Promoted by Permethylzirconocene Dihydride. A Modeling Study of Carbon Monoxide Reduction. *J. Am. Chem. Soc.* **1979**, *101*, 6450–6452.

- (50) Chiu, K. W.; Jones, R. A.; Wilkinson, G.; Galas, A. M. R.; Hursthouse, M. B. Reaction of *tert*-Butyl Isocyanide with Hexamethyltungsten. Synthesis and X-Ray Crystal Structure of WN(Bu^t)CMe₂(Me)(NBu^t){N(Bu^t)(CMe=CMe₂)}. *J. Am. Chem. Soc.* **1980**, *102*, 7978–7979.
- (51) Howard, W. A.; Trnka, T. M.; Waters, M.; Parkin, G. Terminal Chalcogenido Complexes of Zirconium: Syntheses and Reactivity of Cp₂*Zr(E)(NC₅H₅) (E = O, S, Se, Te). *J. Organomet. Chem.* **1997**, *528*, 95–121.
- (52) Howard, W. A.; Waters, M.; Parkin, G. Terminal Zirconium Oxo Complexes: Synthesis, Structure, and Reactivity of (η⁵-C₅Me₄R)₂Zr(O)(NC₅H₄R'). *J. Am. Chem. Soc.* **1993**, *115*, 4917–4918.
- (53) Hanna, T. E.; Lobkovsky, E.; Chirik, P. J. Dihydrogen and Silane Addition to Base-Free, Monomeric Bis(Cyclopentadienyl)Titanium Oxides. *Inorg. Chem.* **2007**, *46*, 2359–2361.
- (54) Fostvedt, J. I.; Grant, L. N.; Kriegel, B. M.; Obenhuber, A. H.; Lohrey, T. D.; Bergman, R. G.; Arnold, J. 1,2-Addition and Cycloaddition Reactions of Niobium Bis(Imido) and Oxo Imido Complexes. *Chem. Sci.* **2020**, *11*, 11613–11632.
- (55) Tomson, N. C.; Arnold, J.; Bergman, R. G. Halo, Alkyl, Aryl, and Bis(Imido) Complexes of Niobium Supported by the β-Diketiminato Ligand. *Organometallics* **2010**, *29*, 2926–2942.
- (56) Trofimenko, S. Recent Advances in Poly(pyrazolyl)borate (Scorpionate) Chemistry. *Chem. Rev.* **1993**, *93*, 943–980.
- (57) Santini, C.; Marinelli, M.; Pellei, M. Boron-Centered Scorpionate-Type NHC-Based Ligands and Their Metal Complexes. *Eur. J. Inorg. Chem.* **2016**, 2312–2331.

- (58) Xiang, L.; Xie, Z. Conversion of $(\eta^5-C_2B_9H_{10}R)TaX_3$ (X = Me, NMe₂) to $(\eta^6-C_2B_9H_{10}R)TaX'$ (X' = NMe₂, Azaallyl) in the absence of a reducing agent: Synthesis and structure of tantallacarboranes incorporating an arachno- $\eta^6-C_2B_9^{4-}$ ligand. *Chem. Commun.* **2014**, *50*, 8249–8252.
- (59) Xiang, L.; Mashima, K.; Xie, Z. Reaction of $[\eta^1:\eta^5-(Me_2NCH_2CH_2)C_2B_9H_{10}]$ TaMe₃ with aryl isonitriles: Tantallacarborane-mediated facile cleavage of C–N multiple bonds. *Chem. Commun.* **2013**, *49*, 9039–9041.
- (60) Macdonald, M. R.; Ziller, J. W.; Evans, W. J. Coordination and Reductive Chemistry of Tetraphenylborate Complexes of Trivalent Rare Earth Metallocene Cations, [(C₅Me₅)₂Ln][(μ-Ph)₂BPh₂]. *Inorg. Chem.* **2011**, *50*, 4092–4106.
- (61) Wahl, G.; Kleinhenz, D.; Schorm, A.; Sundermeyer, J.; Stowasser, R.; Rummey, C.; Bringman, G.; Fickert, C.; Kiefer, W. Peroxomolybdenum Complexes as Epoxidation Catalysts in Biphasic Hydrogen Peroxide Activation: Raman Spectroscopic Studies and Density Functional Calculations. *Chem. Eur. J.* **1999**, *5*, 3237–3251.
- (62) Namorado, S.; Antunes, M. A.; Veiros, L. F.; Ascenso, J. R.; Duarte, M. T.; Martins, A.
 M. Ionic Hydrogenation of Ketones with Molybdenum Pentabenzylcyclopentadienyl Hydride
 Catalysts. *Organometallics* 2008, 27, 4589–4599.
- (63) Otten, E.; Batinas, A. A.; Meetsma, A.; Hessen, B. Versatile Coordination of Cyclopentadienyl-Arene Ligands and Its Role in Titanium-Catalyzed Ethylene Trimerization. *J. Am. Chem. Soc.* **2009**, *131*, 5298–5312.

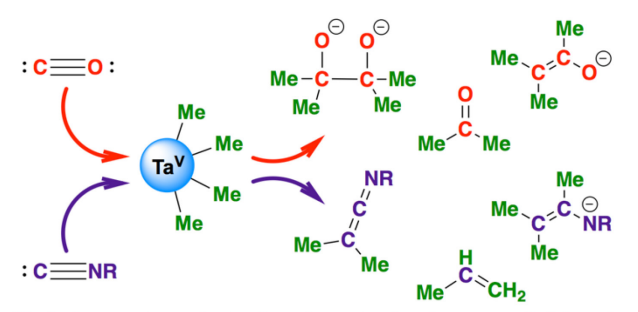
- (64) Giannini, L.; Caselli, A.; Solari, E.; Floriani, C.; Chiesi-Villa, A.; Rizzoli, C.; Re, N.; Sgamellotti, A. Organometallic Reactivity on a Calix[4]Arene Oxo Surface. The Stepwise Migratory Insertion of Carbon Monoxide and Isocyanides into Zirconium-Carbon Bonds Anchored to a Calix[4]Arene Moiety. *J. Am. Chem. Soc.* **1997**, *119*, 9709–9719.
- (65) Martin, B. D.; Matchett, S. A.; Norton, J. R.; Anderson, O. P. Nucleophilic Attack on η²-Acetyl Ligands. Structure of a Bridging η²-Acetone Complex. J. Am. Chem. Soc. 1985, 107, 7952–7959.
- (66) Hessen, B.; Teuben, J. H.; Lemmen, T. H.; Huffman, J. C.; Caulton, K. G. Cyclopentadlenylvanadlum(III) and -Vanadium(II) Methyl, Phenyl, and Borohydride Compounds. *Organometallics* **1985**, *4*, 946–948.
- (67) Galindo, A.; Gómez, M.; Del Río, D.; Sánchez, F. Synthesis and Reactivity of Ene-Diamido and Ene-Diolato [(Trimethylsilyl)-Cyclopentadienyl]Niobium(V) Complexes and a Comparative DFT Study of the Bonding Capabilities of Diazabutadiene and Butadiene Ligands. *Eur. J. Inorg. Chem.* **2002**, 1326–1335.
- (68) Fandos, R.; López-Solera, I.; Otero, A.; Rodríguez, A.; Ruiz, M. J.; Terreros, P. Synthesis and Reactivity of Monocyclopentadienyl Tantalum Complexes with Pincer Dialkoxide Ligands. *Organometallics* **2004**, *23*, 5030–5036.
- (69) Goldberg, K. I.; Bergman, R. G. Synthesis of Dialkyl- and Alkylacylrhenium Complexes by Alkylation of Anionic Rhenium Complexes at the Metal Center. Mechanism of a Double Carbonylation Reaction That Proceeds via the Formation of Free Methyl Radicals in Solution. *J. Am. Chem. Soc.* **1989**, *111*, 1285–1299.

- (70) Crestani, M. G.; Hickey, A. K.; Gao, X.; Pinter, B.; Cavaliere, V. N.; Ito, J. I.; Chen, C. H.; Mindiola, D. J. Room Temperature Dehydrogenation of Ethane, Propane, Linear Alkanes C4-C8, and Some Cyclic Alkanes by Titanium-Carbon Multiple Bonds. *J. Am. Chem. Soc.* **2013**, *135*, 14754–14767.
- (71) Du, G.; Mirafzal, G. A.; Woo, L. K. Reductive Coupling Reactions of Carbonyl Compounds with a Low-Valent Titanium(II) Porphyrin Complex. *Organometallics* **2004**, *23*, 4230–4235.
- (72) Xu, X.; Hirao, T. Vanadium-Catalyzed Pinacol Coupling Reaction in Water. *J. Org. Chem.* **2005**, *70*, 8594–8596.
- (73) Obora, Y.; Kimura, M.; Tokunaga, M.; Tsuji, Y. Low-Valent Nb(III)-Mediated Synthesis of 1,1,2-Trisubstituted-1*H*-Indenes from Aliphatic Ketones and Aryl-Substituted Alkynes. *Chem. Commun.* **2005**, 901–902.
- (74) Takai, K.; Kataoka, Y.; Utimoto, K. Tantalum-Alkyne Complexes as Synthetic Intermediates. Stereoselective Preparation of Trisubstituted Allylic Alcohols from Acetylenes and Aldehydes. *J. Org. Chem.* **1990**, *55*, 1707–1708.
- (75) Okuda, J.; Herberich, G. E. Reactivity of a Labile Molybdenocene Olefin Complex With Organic π-Acceptors. *Organometallics* **1987**, *6*, 2331–2336.
- (76) Chisholm, M. H.; Folting, K.; Klang, J. A. Reaction between Benzophenone and Ditungsten Hexaalkoxides. Molecular Structure and Reactivity of W(OCH₂-t-Bu)₄(Py)(η²-OCPh₂). Organometallics **1990**, *9*, 607–613.

- (77) Mcmurry, J. E. Carbonyl-Coupling Reactions Using Low-Valent Titanium. *Chem. Rev.* **1989**, 89, 1513–1524.
- (78) Stahl, M.; Pidun, U.; Frenking, G. On the Mechansim of the McMurry Reaction. *Angew. Chem., Int. Ed.* **1997**, *36*, 2234–2237.
- (79) Beaumier, E. P.; Pearce, A. J.; See, X. Y.; Tonks, I. A. Modern Applications of Low-Valent Early Transition Metals in Synthesis and Catalysis. *Nat. Rev. Chem.* **2019**, *3*, 15–34.
- (80) Gianetti, T. L.; Nocton, G.; Minasian, S. G.; Tomson, N. C.; Kilcoyne, A. L. D.; Kozimor, S. A.; Shuh, D. K.; Tyliszczak, T.; Bergman, R. G.; Arnold, J. Diniobium Inverted Sandwich Complexes with μ-η⁶:η⁶-Arene Ligands: Synthesis, Kinetics of Formation, and Electronic Structure. *J. Am. Chem. Soc.* **2013**, *135*, 3224–3236.
- (81) Kriegel, B. M.; Naested, L. C. E.; Nocton, G.; Lakshmi, K. V.; Lohrey, T. D.; Bergman, R. G.; Arnold, J. Redox-Initiated Reactivity of Dinuclear β-Diketiminatoniobium Imido Complexes. *Inorg. Chem.* **2017**, *56*, 1626–1637.
- (82) Škoch, K.; Císařová, I.; Štěpnička, P. Selective Gold-Catalysed Synthesis of Cyanamides and 1-Substituted 1*H*-Tetrazol-5-Amines from Isocyanides. *Chem. Eur. J.* **2018**, *24*, 13788–13791.

SYNOPSIS. We present the reactivity of Ta(V) methyl complexes toward unsaturated substrates under mild reaction conditions to yield a variety of products containing newly-formed C-C bonds. We demonstrate conversion of CO and CNXyl into higher-value products, including enols, enamines, imines, ketenimines, propene, and acetone, via successive methyl transfers from Ta centers. Notably, we report and study the mechanism of pinacol formation from CO and Ta-methyl groups, a new reaction pathway in the early transition metal literature.

TABLE OF CONTENTS GRAPHIC.



Methyl group transfer to C₁ substrates leads to new C-C bonds